



International Association of Geomorphologists  
Association Internationale des Géomorphologues



6 -11 November 2017 | Vigyan Bhawan, New Delhi, India

Organised by  
Indian Institute of Geomorphologists (IGI)

## B6: Geomorphological Field Guide Book on SEMI-ARID GUJARAT ALLUVIAL PLAIN

### Convener

**L.S. Chamyal and D.M. Maurya**

Department of Geology, Faculty of Science  
The M.S. University of Baroda, Vadodara

### Series Editor

**Amal Kar** (Kolkata)

Formerly of Central Arid Zone  
Research Institute (CAZRI), Jodhpur

New Delhi, 2017



**Published by:**

Indian Institute of Geomorphologists (IGI),  
Allahabad

**On the occasion of:**

9th International Conference on Geomorphology  
of the International Association of Geomorphologists (IAG),  
New Delhi (6-11 November, 2017)

**Citation:**

Chamyal, L.S. and Maurya, D.M. 2017. *Geomorphological Field Guide Book on Semi-arid Gujarat Alluvial Plain* (Edited by Amal Kar). Indian Institute of Geomorphologists, Allahabad.

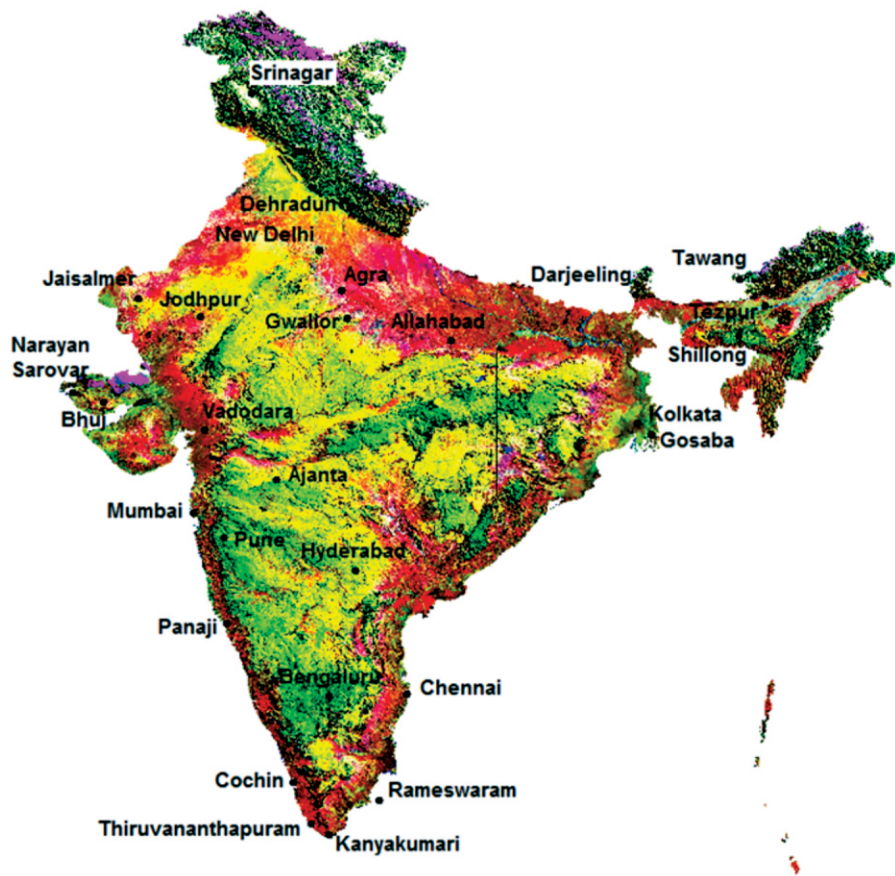


Fig. 1. Image-map of India, showing some places of interest for the 9th International Conference on Geomorphology, 2017 (Map prepared by A. Kar through processing of relevant ETM+ FCC mosaics and SRTM 1km DEM, both sourced from the USGS site). Boundaries are approximate.

**Geomorphological Field Guide Book on  
Semi-arid Gujarat Alluvial Plain  
(12 November to 16 November, 2017)**

**Itinerary**

<b>Day</b>	<b>Date</b>	<b>Places from - to</b>	<b>Stay</b>
Day 1	12 November 2017	New Delhi to Vadodara by Flight; Briefing and discussion	Vadodara
Day 2	13 November 2017	Field visit for geomorphology and late Quaternary sequences of Mahi River basin: Vadodara to Rayka, Kothiyakhad, Mujpur and Dabka, and back	Vadodara
Day 3	14 November 2017	Field visit for geomorphology and late Quaternary sequences of the lower Narmada River basin Vadodara to Gamod, Tilakwada, Chandod and Phulwadi, and back	Vadodara
Day 4	15 November 2017	Field visit for tectonic geomorphology in the Narmada-Son Fault (NSF) zone Vadodara to Juna Ghanta, Nava Ghanta (along the Nandikhadi River), Khojalwasa, Tejpur and Karjan dam, and back	Vadodara
Day 5	16 November 2017	Field visit for estuarine sequences of the Narmada River Vadodara to Tavra, Bharuch, Ranipura and Karad, and back to Vadodara Departure from Vadodara to New Delhi by evening flight	New Delhi



## A. GUJARAT AND ITS ALLUVIAL PLAIN: AN INTRODUCTION

The state of Gujarat, located astride the Tropic of Cancer, and to the south of the Thar Desert of Indian subcontinent, forms an important part of the drylands of western India. The climate of the state is dominantly semi-arid, but the northernmost part in Kachchh and Banaskantha has an arid climate, while the southernmost part experiences a sub-humid climate. Winter is mild, pleasant and dry in the state. The average daytime temperatures is around 29°C (84°F) and night temperature is about 12°C (54°F), with sunny days and clear nights. Summer is extremely hot and dry when day temperatures usually rises to 45°C (120°F), while night temperature reaches about 30°C (86°F). In the weeks leading to the arrival of the southwest monsoon rains by mid-June, the high temperature gets associated with high humidity, making the condition very oppressive. As the rains arrive the temperature drops to below 35°C. Rainy season continues till the end of September, and often causes flood in many areas. The rest of the months receive almost no rainfall.

Physiographically, Gujarat can be divided into the following three well-defined zones: Mainland Gujarat, Saurashtra, and Kachchh peninsula (*Fig. 2*). These three zones correspond well with the three distinct tectonic provinces of western India (*Fig. 3*). The geological set up of the state is a result of complex interaction between tectonism and sea level changes during the Cenozoic. The basic framework was formed due to sequential fragmentation of the western continental

margin of the Indian plate during Late Mesozoic, as it collided with the Eurasian plate in the north (Biswas, 1987). The break up of the margin resulted in the formation of the Kachchh, Cambay and Narmada rift basins along the Satpura, Dharwar and



*Fig. 2.*  
*Physiographic zones in  
Gujarat state and sites to be visited.*

Narmada trends (Biswas, 1987). These basins have been the major depo-centers of western India since then and furnish classical examples of sedimentation in tectonically controlled environment. While a major part of Tertiary sediments in these basins is of marine origin, the Quaternary sedimentation has been largely fluvial (Merh, 1993).

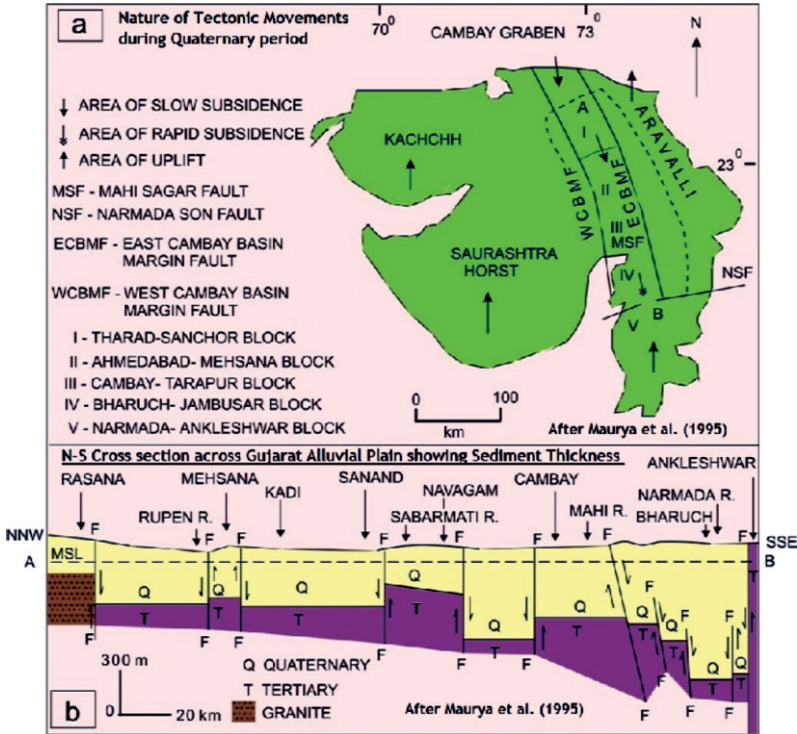


Fig. 3.

(a) Map of Gujarat showing the nature of tectonic movements during Quaternary.

(b) N-S cross section across the Gujarat alluvial plain showing the variable thickness of Quaternary sediments (after Maurya et al., 1995).

## Geomorphology of the Gujarat Alluvial Plain

Mainland Gujarat can be divided into four broad geomorphic zones: the eastern upland zone, the shallow buried pediment zone, the alluvial zone and the coastal zone (Maurya et al., 2000). The flat alluvial plain, called the Gujarat Alluvial Plain, is bordered by the Aravalli ranges and the Trappean highlands to its east (*Fig. 3a*), and occupies a major part of Mainland Gujarat. Its subsurface cross section brings out the influence of tectonic framework of the Cambay and the Narmada basins, and their various tectonic blocks, on Quaternary sedimentation within the plain (*Fig. 3b*). The basin is composed of a series of horsts and grabens from the Tertiary period, which are subjected to periodic uplifts and subsidence, but overall the basin is subsiding. The plain shows a gentle slope towards SW.

### Fluvial system

The landscape of the area has evolved due to tectonic activities and other palaeo-environmental changes during the late Quaternary period (Maurya et al., 2000; Chamyal et al., 2003). The streams of Mainland Gujarat originate in the eastern highlands and debouch into the Gulf of Cambay. The Sabarmati, the Mahi and the Narmada are the major rivers draining the alluvial plains (*Fig. 4*). All the rivers of the alluvial plains are characterised by gorge-like valleys with 30-50 m high vertical cliffy banks, associated deep ravines, presence of tributaries on one bank only, deeply entrenched meanders, and slope-deviatory approach of several rivers. All these features suggest an influence of tectonism.

Lineament analysis has revealed a strong control of tectonic elements in the drainage configuration (Maurya et al., 2000). The lineaments correspond to three major structural trends, NE-SW, ENE-WSW and NNW-SSE, which parallel the Aravalli, Satpura and Dharwar regional trends, respectively (*Fig. 4*). The Dharwar trend is found to dominate in the northern and central part, where the Aravalli trend is present as the second major trend. The Satpura trend dominates the southern part. The N-S and NNW-SSE lineaments seem to reflect the basin configuration, while drainage courses of the area follow NE-SW and NNE-SSW lineaments (Maurya et al., 2000).

The NNW-SSE and ENE-WSW lineaments (*Fig. 4*) correlate well with the subsurface intra-basin horsts and grabens in the northern alluvial plains (Maurya et al., 2000). The ENE-WSW to E-W trend suggests the subsurface continuation of the Aravallis. The area south of Mehsana and up to Sabarmati River is devoid of basement highs, which diverts the streams like the Sabarmati River to flow towards the south. To the south of Sabarmati River, a NE-SW to NNE-SSW subsidiary trend is seen in addition to the dominant trend. The eastern margin fault is represented by a series of sub-

parallel en-echelon lineaments trending in N-S and NNW-SSE directions (Fig. 4). The lineament density on the eastern margin is higher as compared to that on the western margin. Near Narmada River the NE-SW lineament is replaced by a ENE-WSW lineament, suggesting an influence of the Narmada-Son Fault (Fig. 4). South of the Mahi River a major lineament trending NNE-SSW controls the extent of ravines along that river, as also the course of the Vishwamitri River. An E-W trending lineament along the Mahi estuary marks the Mahisagar Fault in the subsurface.

The lineament rosettes for the northern, central and southern alluvial plains show a change from N-S orientation in the northern plains to ENE-WSW in the southern plains (Fig. 4 A, B, C). In the northern plains, the N-S Cambay basin trend is dominant whereas in the central plains, a gradual swing towards the east is observed because of the increasing influence of the NE-SW Aravalli trend. In this part, the NNW-SSE and NNE-SSW trends dominate. In the southern plains, the major lineaments trend ENE-WSW, parallel to the Narmada trend (Maurya et al., 2000). Lineaments parallel to the Cambay trend are less common.

As suggested above, the drainage architecture of the Gujarat Alluvial Plain reveals a strong structural control (Fig. 5), with excellent correlation with the subsurface structural highs and faults (Maurya et al., 2000). Several areas are devoid of significant drainage lines, viz. to the west of the Sabarmati River, between the lower courses of the Sabarmati and the Mahi rivers, in the lower courses of the Mahi and the Dhadhar rivers, to the west of the lower course of the Orsang River, and to the south of Narmada River (Fig. 5). Such areas correspond well with the subsurface structural highs (Maurya et al., 2000). Several anticlines are present to the south of the Narmada River, causing a northward shift of the course of the river (Fig. 5);

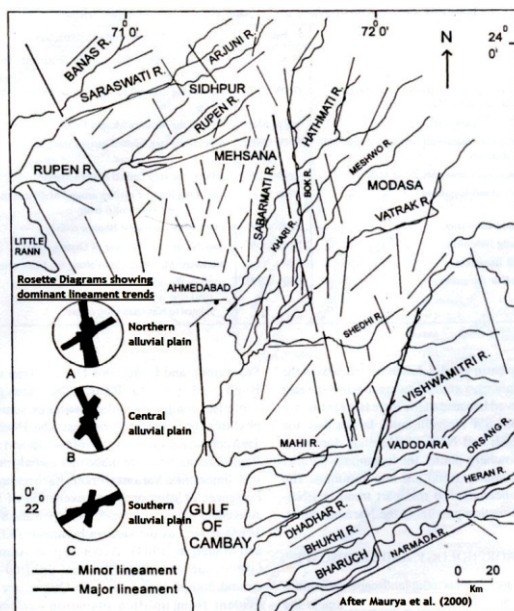


Fig. 4.  
Lineament map of Gujarat alluvial plains  
(after Maurya et al., 2000).

Maurya et al., 2000; Chamyal et al., 2002). The courses of the Sabarmati, the Mahi and the Orsang do not follow the SW regional slope of the plains. According to Maurya et al. (2000), the N-S to NNE-SSW segments of these three rivers appear to have captured the E-W to ENE-W

SW courses of their tributaries which follow the regional slope. The Sabarmati has captured the course of the Vatrak, while the Mahi has captured the course of the Mini, Mesri and Goma rivers, and the Orsang has captured the course of the E-W flowing Heran and Unch rivers. Maurya et al. (2000) also envisaged a phase of drainage realignment during which large-scale river capture took place by the structurally-controlled major rivers. Some rivers, however, show a tendency to flow along or parallel to the basin axis, but an axial drainage consistent with the basin axis is absent in the plains.

Three distinct geomorphic surfaces could be noticed in the landscape in and around the major river valleys of Mainland Gujarat (Maurya et al. 2000). These are: the alluvial plain (S1), the ravine surface (S2) comprising Late Pleistocene sediments, and the Mid-Late Holocene valley fill terrace (S3). The sediments comprising these surfaces have great bearing on the evolutionary history of Mainland Gujarat during the Late Pleistocene and the Holocene.

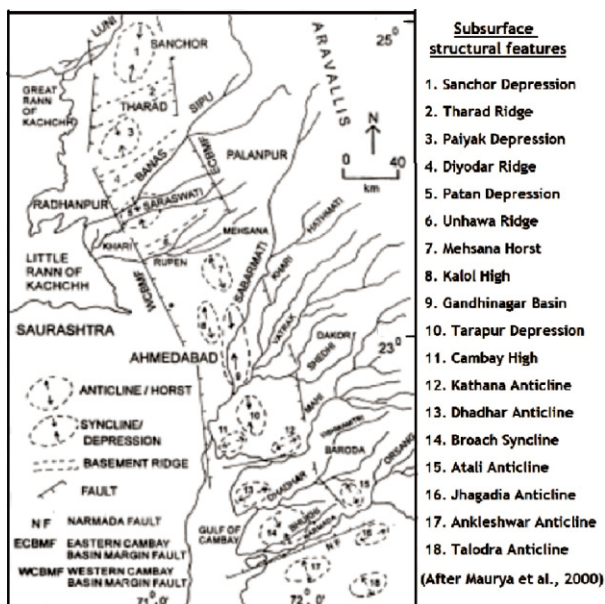


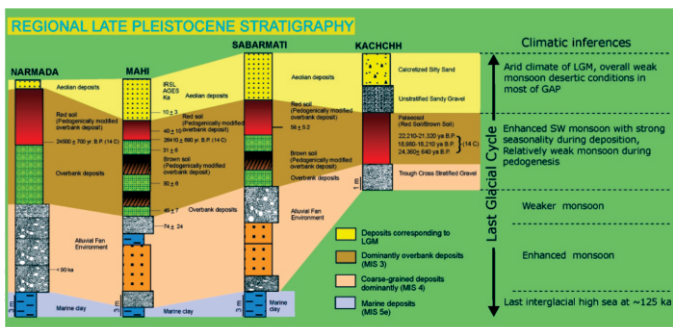
Fig. 5.

*Drainage and subsurface structures in the Gujarat alluvial plain (after Maurya et al., 2000).*

### Regional Stratigraphy of the Exposed Quaternary Sediments

The 30-40 m high alluvial cliffs all along the valleys of the Mahi, the Sabarmati and the lower part of the Namada expose late Pleistocene sediments dating back to ~125 ka BP (Maurya et al., 2000). The exposed succession begins with fine clayey silt that becomes fluvio-marine silty clay in areas proximal to the coast (Fig. 6). This is overlain by cross-stratified gravel. A silty sand horizon with bedded calcrete overlies the gravel, which is overlain either by gritty sand or assorted gravels. Upward in the sequence lies the pedogenically modified silty sand. The uppermost pedogenically modified horizon shows reddening (red soil) that has been used as inter-basin stratigraphic marker. With exception of a few localities where the red soil is overlain by cross-stratified gravel, in majority of cases a weak to moderate pedogenically modified silty sand horizon overlies the red soil (Fig. 6). This horizon grades either into fluvio-aeolian sand or fining upward channel sand. The sequence above red soil has been designated as the upper fluvial sequence (Srivastava et al., 2001; Juyal et al., 2006). This is overlain by aeolian sand that constitutes the topmost litho-unit in the region.

Presence of fluvio-aeolian sediments suggests that the transition from fluvial to aeolian phase was gradual. After ~25 ka, the fluvial regime began to dwindle as indicated by the fining upward channel sand. The establishment of a e o l i a n



Exposed Late-Pleistocene sediments (S1 and S2 surfaces) along the valleys of the lower Narmada, the Mahi, and the Sabarmati in mainland Gujarat, and along the valleys of the rivers in Kachchh. Note the correlation of the major aggradational phases during inferred climatic phases. Lithology based on Chamyal et al. (2002) and Maurya et al. (2003); and the dates are from Allichin et al. (1978), Juyal et al. (2000) and Tandon et al. (1997).

Fig. 6. Exposed late Pleistocene stratigraphy along the Gujarat streams.

sedimentation followed this. Since the controlling factors for aeolian sedimentation are the wind strength and the moisture/vegetation cover, it is suggested that aeolian activity began with the weakening of southwest monsoon around LGM (~ 20 ka). In the dry sub-humid Orsang basin, aeolian sedimentation terminated after the LGM, but in the semi-arid Mahi basin it continued till around 11 ka. Further north, in the Sabarmati basin, aeolian sedimentation continued till 5 ka (Juyal et al., 2003). This shows a gradual northward propagation of aeolian activity, and suggests a moisture-vegetation control on the aeolian dynamics (Juyal et al., 2003).

## Socio-economic Aspects

### Population Density

Gujarat is one of the most industrialized states of India and thus attracts people from India both in terms of investment and jobs. From 50,671,017 in 2001, the population of Gujarat has gone to 60,383,628 in 2011. In terms of population, Ahmedabad is the largest city of Gujarat with 6.2 million people living here. Surat and Vadodara are other two major cities with high number of urban population residing here. Rajkot is the fourth largest city of Gujarat with population of 1.50 million. The cities like Bhavnagar, Bhuj, Junagadh and Jamnagar constitutes a large number of urban populations in Gujarat. Population in Gujarat is growing at an annual growth rate of 1.9 percent.

Gujarat has also shown an increase in its literacy rate by 10 percent in this decade. Currently it stands at 79.31 percent as compared to last census (2001) figures of 69.14 percent. Better education facilities by the state government have proved a vital role in improving overall literacy rate of Gujarat. According to latest Census of 2011, Male Literacy rate in Gujarat stands at 87.23 percent while female literacy rate is 70.73 percent.

### Agriculture

Gujarat is the main producer of tobacco, cotton, and groundnuts in India. Other major crops produced are rice, wheat, jowar, bajra, maize, tur, and gram. Gujarat has an agricultural economy; the total crop area amounts to more than one-half of the total land area. Animal husbandry and dairying have played a vital role in the rural economy of Gujarat. Dairy farming, primarily concerned with milk production, functions on a cooperative basis and has more than a million members. Gujarat is the largest processor of milk in India. Amul milk co-operative federation products are well known all over India and is Asia's biggest dairy. Among livestock raised are buffalo and other cattle, sheep, and goats. As per the livestock census, there were 20.97 million livestock in Gujarat state in 1997. As per the estimates of the survey of major livestock products, during the year 2002–03 the Gujarat produced 6.09 million tonnes of milk, 385 million eggs and 2.71 million kg of wool. Gujarat also contributes inputs to industries like textiles, oil and soap.

### **Vadodara - Educational and Cultural Heritage**

Sir Sayaji Rao Gaekwad III, the late ruler of Vadodara had a dream to make Vadodara an educational, industrial and commercial centre. He ensured that his dream came true. The city of Vadodara has a long history. The first noted history of the city was of the early traders who settled here in 812 AD. The city afterwards came under the Gupta dynasty, and then under the Chalukya dynasty and the Solanki dynasty. It then was captured by the Delhi Sultans, and subsequently by the Mughals. Since the city was a known seat of trade and commerce with international connectivity, Vadodara always remained a prized possession of the rulers of India. During the Mughal Period the Marathas of the Deccan region became more powerful, and eventually they took control of Vadodara and its large hinterland. Vadodara then became the capital of the Maratha Gaekwad, and remained so till independence of India in 1947.

Vadodara is now the third largest state in Gujarat, and is famous for its rich culture and heritage. The inhabitants love to tell the visitors that their city is a 'Sanskari Nagari', i.e., a 'cultured city'. Diwali, Uttarayan, Holi, Eid, Gudi Padwa and Ganesh Chaturthi are celebrated here with great fervour. Vadodara is also famous for 'Garba' dance, which is performed all across Gujarat during the nine-day Durga Puja festival, the 'Nava-Ratri' celebration. The city has several places of tourist interest, which include the Laxmi Vilas Palace, Baps Swaminarayan temple, EME Temple, Baroda Museum and Picture Gallery, Sayaji Baug, etc. Vadodara is also known for its art and architecture. Under the patronage of the royal Gaekwad family since 19th Century, Vadodara became a hub of art and architecture. The city is also known as the 'Kala Nagari'.

### **Ahmedabad - Educational and Cultural Heritage**

Ahmedabad, once termed as India's Manchester, is one of the oldest cities in India. The city now dreams to get recognition as one of the World's Heritage Cities. It has been witness to some of India's historic events. It was from this city that Mahatma Gandhi started his Dandi March. Ahmedabad is a city that boasts of a vibrant walled city which has generated much interest all over the world. It's a city where history gently rubs its shoulders with modernity.

Apart from the Indo-Islamic architecture for which Ahmedabad is quite well known, there are almost 100 Jain temples in the old city, some of which are architectural wonders from Medieval Gujarat. The old city within the walls with designated gates (or the 'Pols') has many traditional houses, which capture the essence of community living, and are unique to Ahmedabad. So are the 'chabutras', or the open spaces in between a cluster of houses, or even a large courtyard in a building complex, which is designated for feeding the birds. Such traditional systems throw light on the peaceful

living style of the inhabitants of the city. Ahmedabad has played a vital role in the independence movement of the country. Unlike many other glorious cities across the globe that have lost their relevance and distinct character, Ahmedabad has kept its past alive and looks forward to a promising future. Many other Indian cities have taken lessons from Ahmedabad on conservation of heritage. The city also boasts of a Heritage Walk which takes the visitors through the lanes and by-lanes of history. Architects, planners and heritage conservationists agree that Ahmedabad is a "living heritage city" where the walled city planning system is based on the ancient traditional "Vaastu" principles. The sharing of community spaces and resources such as water and building structure, techniques and materials, offers social security and self-sufficiency to the 'pol' inhabitants.

## B. DESCRIPTION OF THE FIELD SITES

### **Day 1: 12/11/2017**

#### **New Delhi to Vadodara by Flight**

#### **Discussion on the logistics**

#### **Stay at Vadodara.**

On the first day, the delegates will arrive from New Delhi to Vadodara by flight. The programme for the day includes an informal gathering for a briefing on the day-wise schedule of the field trip, as well as for a discussion on the general geological and geomorphological characteristics of the Gujarat Alluvial Plain.

### **Day 2: 13/11/2017**

#### **Vadodara to Rayka, Kothiyakhad, Mujpur, Dabka in Mahi River basin and back**

#### **Stay at Vadodara.**

It is proposed to begin the field trip in Gujarat Alluvial Plain with an excursion to the Mahi River basin. To appreciate the landscape better and to understand the geomorphology of the area, we first provide a short review of the tectono-morphic setting of the basin and its importance in the late Quaternary evolutionary history of the landforms.

### **Geomorphology and Late Quaternary Sequences of Mahi River Basin**

The Mahi River basin is the third largest river basin in Gujarat, after the Narmada and the Tapi River basins. The Mahi River originates in the Aravalli hills and flows along the eastern flank of the Cambay Graben, which is an intra-cratonic rift graben (Biswas, 1987). It then flows through its alluvial plain before debauching into the Gulf of Cambay. The East Cambay Basin Margin Fault (ECBMF) cuts across the Mahi River, as indicated by a change in orientation of the river (Maurya et al., 1997a). Several N–S and NNW–SSE trending fractures that developed parallel to the ECBMF have strongly influenced the drainage pattern in the basin (Maurya et al. 1997a; Pant and Chamyal, 1990). Thus, whenever the Mahi approaches a lineament it deviates from its NE–SW path to take a NNE–SSW course. Subsurface data indicate the presence of pre-existing step faults parallel to the ECBMF that acted as the depo-centre for late Pleistocene sedimentation (Maurya et al. 1995; 1997a). The Mahi basin lies in a horst segment, which has more than 300 m of Quaternary sediments overlying the Tertiary rocks (Maurya et al. 1995). The geomorphic features of the basin indicate a complex interplay of tectonism and base level changes in its evolution (Maurya et al. 1997a; Pant and Chamyal, 1990). Two distinct geomorphic zones are identified here.

The first zone, identified as the rocky upland zone, is characterized by high, steep, rocky hill slopes with deep and narrow stream valleys having steep longitudinal profiles. This zone has been rejuvenated during the Quaternary period (Sen and Sen, 1983; Ahmad, 1986). The second zone is the alluvial zone, where the Pleistocene-Holocene alleviation took place. The landscape here is dominated by wide valleys, but also includes extensive badlands that suggests active denudational processes related to Holocene tectonic uplift (Raj et al. 1999). The Mahi River has carved out a conspicuous entrenched meandering course across the alluvial plain. Two distinct land surfaces, an older ( $S_1$ ) and a younger ( $S_2$ ), can be demarcated from the different geomorphic features along the Mahi River (Maurya et al., 1997b). The  $S_1$  is an old, pre-Holocene surface, and is paired, highly eroded and extensively dissected, comprising of sand, silt and gravel, mainly of fluvial and aeolian origins. The  $S_2$  is the younger Holocene surface, which occurs as unpaired elevated terraces, comprising of two lithofacies: (a) the tidal estuarine mud and sand, and (b) the fine to medium sand of mixed environment. Two phases of tectonic uplift and fluctuating sea-level have helped in shaping the landscape of the lower Mahi valley (Maurya et al., 1997b).

An observation of the  $S_2$  surface shows that the sequence commences with the deposition of marine clay (Raj et al., 1998), with evidence of intense pedogenesis (Khadkikar et al., 1998). It is overlain by a planar cross-stratified gravel bed (Gravel-1). This is succeeded by a sandy layer with mud drapes and bedded calcretes. Trough

cross-bedded gravel (Gravel-2) overlies this, which in turn is overlain by two to three pedogenised horizons, the uppermost being red in color (red soil). The red soil is overlain by medium to fine-grained fluvial sand that becomes fluvio-aeolian in character in the upper part. The aeolian sand sheet finally blankets the succession (Fig. 7). At Rayka, the aeolian sand sheet directly overlies the red soil. However, recent

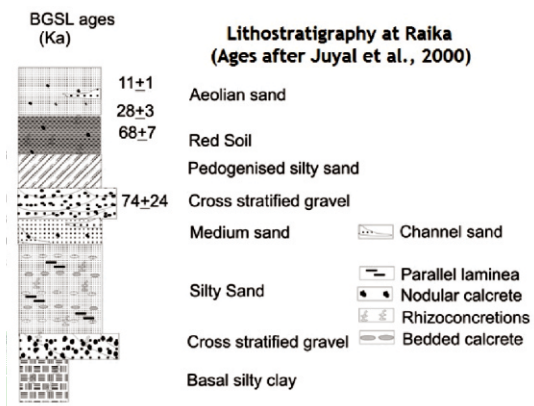


Fig. 7.

Lithostratigraphic succession exposed at Rayka with BGS L ages (after Juyal et al., 2000).

investigations in the lower reaches of the Mahi basin indicated that a renewed phase of fluvial aggradation followed the development of red soil. This event has been

designated as the upper fluvial sequence (Srivastava et al., 2001, Juyal et al., 2006), which gradually merges upwards into the aeolian sediments.

Proximity of the Mahi basin to the Gulf of Cambay and presence of marine clays at the base of the exposed sections suggest eustatic control on sedimentation. The overlying fluvial aggradation was consequent to base level changes following marine regression. During this phase, the river could erode and transport sediments from poorly vegetated catchment (Graf, 1988). Presence of basalt and carbonate concretions in Gravel-1 indicates poorly vegetated source (proximal catchment). The silty sand with bedded calcretes overlying Gravel-1 suggests cohesive banks and persistent flow (sinuous stream) with periods of dryness resulting in the formation of bedded calcretes (McCarthy and Metcalf, 1990). Dominance of poorly-sorted clasts of calcrete, quartzite and basalt in Gravel-2 indicates substantial flow intensities. Rolled carbonate nodules further indicate the ability of flow to erode pre-existing alluvial carbonate under frequent channel migration. The textural evidences suggest the existence of ephemeral fluvial system during the deposition of Gravel-2. Fine sand, silt and clay that have been pedogenised, dominate the overlying sediments. These form laterally extensive sand sheets. Higher concentration of silt indicates that deposition occurred away from the main channel on the flood plain by the meandering stream (Juyal et al., 2000). Presence of pedogenic horizons suggests periods of alluviation, followed by prolonged periods of pedogenesis. Out of the three horizons, the uppermost is red in colour, whereas the lower two are grey in colour. Generally, the red soils develop on better drained sites, reflecting higher elevation and/or more permeable parent material, whereas the grey flood plain soils are formed in poorly drained areas with less permeable material (Kraus, 1997).

Following the development of red soil, climate temporarily reverted back to drier conditions as indicated by the overlying trough cross-stratified sandy gravel. However, this event was short-lived and localized. Discrete occurrence of planar and cross-stratified gravel dominated by poorly sorted clasts of basalt, quartzite and calcrete at Dodka, Jaspur and Sultanpur, suggests sudden increase in sediment supply. This could happen in arid and semi-arid environment where episodic storm surge events are common, during which rivers are capable of eroding and transporting sediments from poorly vegetated catchment (Graf, 1988). This gives rise to braided channel system having typically large width to depth ratio in which the number of individual channels can vary from 1 to more than 20 (Thornes, 1994). In a rare event the river bed is completely occupied. However, in a given time the distributary channels carry water and are known for frequent migrations that lead to bank erosion. In view of limited extent of such features, it can be suggested that the event was short-lived and local in nature.

A persistent fluvial regime reappears in the basin with the deposition of fine silty sand, usually overlying the red soil. Distinct fluvial signatures are preserved in the form of current ripple laminations and mud balls, suggesting prevalence of a low-energy meandering river system. The deposits are typical of flood plain fine facies of Miall (1996), representing the sedimentation in a flood plain regime (Willis and Behrensmeyer, 1994). These sediments are at times associated with the bedded calcrete at places like Jaspur and Dahewan. Bedded calcrete formation is usually related to the groundwater fluctuation in a riverine playa environment (Goudie, 1983), thus suggesting its deposition proximal to a channel. It has been suggested that in semi-arid areas the flood plains are most conducive locations for the development of bedded calcretes where groundwater remains close to the surface, ensures high evaporation, and facilitates calcrete development (McCarthy and Metcalf, 1990). A vertical aggradation of this facies, ranging in thickness from 2-10 m, suggests that the deposition was facilitated under a persistent flow regime under a well-defined channel (e.g. meandering course) with periodic over-spilling of silty sand on to the adjacent floodplains. Evidence of moderate pedogenesis associated with these sediments suggests phases of non-deposition when the channel responsible for the flood plain aggradation migrated laterally. Such channel migration occurs under changing water budget (both increasing and decreasing). In either situation, river tends to abandon the old course and occupies the new one. This leads to the exposure of the flood plain sediments to sub-aerial weathering and the development of flood plain soils (Kraus and Aslan, 1993). It is evident that the sediments above the red soil were deposited under improved moisture availability. The overlying aeolian sand shows gradational contact with the underlying fluvial horizon. This indicates initiation of drier climatic condition, which could be associated with enhanced wind activity in the region.

Juyal et al. (2000) provided the chronology for the exposed Late Quaternary sequence at Rayka that is considered to be the type locality in the Mahi basin. The basal marine clay was assigned the Marine Isotopic Stage-5 (MIS-5). Gravel-1 and 2 were deposited between the MIS-5 and 74 ka and the silty sand with intercalated pedogenised horizons were formed between 74 ka and 40 ka. However, recent chronometric data based on Quartz extract on red soil at Jaspur suggest that the sequence overlying the red soil could have developed between 68 ka and 50 ka. Thus, the earlier age of  $40 \pm 10$  ka on red soil obtained on feldspar mineral at Rayka probably suggests an age underestimation due to fading, a phenomenon associated with feldspar dating (Juyal et al., 2000). Since luminescence dating gives the sediment deposition ages, hence it can be inferred that red soil development postdates 68 ka (age of red soil sediment) and pre-dates 50 ka (age of the overlying fluvial sand), and probably represents the Marine Isotopic Stage-4.

The overlying fluvial and fluvio-aeolian sediments (upper fluvial sequence) are bracketed between  $50 \pm 8$  and  $34 \pm 3$  ka (MIS-3). Presence of bedded calcretes in the upper fluvial sequence dated to MIS-3 indicates that fluvial activity was not monotonous but punctuated by fluctuating hydraulic discharge. Towards the upper part, dominance of very fine sand indicates that there was a subordinate aeolian component getting admixed with the weak fluvial regime. Finally, the drier conditions set in around 30 ka, as indicated by the initiation of aeolian sedimentation.

### Stop 1: Rayka Section

The Rayka section is located 20 km NW of Baroda on the eastern flank (left bank) of Mahi River. It exposes a 40 m high alluvial cliff. The section has been considered as a type section and documents a sequence of the palaeoclimatic variation over the past  $\sim 125$  ka (Fig. 7). The exposed succession shows two distinct phases of fluvial aggradation. The earliest is located between Gravel-1 and Gravel-2 in the form of sandy calcareous (62% sand) unit. This is followed by the second phase, which is represented by a sandy silt (59% sand) unit, intercalated with palaeosols lying above Gravel-2. The stratigraphic succession of the deposit commences with a clay bed containing shallow marine microfauna, which is overlain by planar cross-stratified Gravel-1. The clay has yielded fairly rich assemblage of foraminiferids, comprising benthic foraminiferids (Rachna Raj et al., 1998) like *Pararotalia* sp., *Brizalina* spp., *Nonion* spp., *Cibicides* spp., *Florilus* spp., *Ammonia* spp., and three species of planktonic foraminiferids, viz., *Turborotalia* sp., *Globigerina bulloides* (Parker, Jones and Brady) and *Globigerinoides ruber* (d'Orbigny). On the basis of the foraminiferids, it has been concluded that the formation was deposited in an estuarine to marginal marine environment, having low salinity due to influx of fresh water during Late Pleistocene. The marine clay is yellowish brown (10 YR 5/4) to brown (7.5 YR 5/4)

and is highly pedogenised. The exposed thickness of the unit ranges from 0.5m to 3.0 m, but extends to a depth of 25 m below mean sea level at Rayka (Murthy, 1975). The unit shows intense fracturing with intersects, giving rise to subangular cohesive blocky aggregates, as also continuous concave upward planes, which can be interpreted as pseudo-anticlines (Fig. 8). Calcium carbonate is dispersed irregularly



Fig. 8.  
Close view of vertisol, showing  
pseudo-anticline and  
other vertic characters at Rayka.

throughout the clays, both as nodules and tubes (*Fig. 8*). The clay mineral assemblage (Malik et al., 1999) is dominated by a very high percentage of smectite (montmorillonite), with subordinate quantities of illite and kaolinite. Presence of shallow marine foraminifera in the clays suggests that they were deposited during a high-sea strand corresponding to a pluvial climate.

The cross-bedded gravel that overlies the marine clay with an erosional contact indicates initiation of fluvial activity. Well-developed 2-3 m thick planar-cross stratification in the gravels, comprised of basalt fragments and carbonate nodules, indicate proximal source. Planar cross-stratification (1 m) is commonly associated with ephemeral flow and is often formed by an advancing channel bar. The presence of associated clay drapes indicates the recession of the flood peaks during which clay particles settle out. Thus, the Gravel-1 was perhaps deposited during the peak flood events when large volumes of wash load and bed load were eroded from poorly vegetated slopes.

This unit is overlain by laminated sandy silt with carbonates in discrete bands or as irregular nodules. Nearly 50 such layers are recorded, which occur at regular intervals. The composite thickness of these laterally traceable layers varies between 3 and 5 m. No significant pedogenesis has been found to be associated with these layers, which could be due to syn-depositional tectonism, as indicated by soft-sediment deformation structures (Maurya et al., 1997; Jain et al., 1998). Textural characteristics and consistency in the appearance of the individual layers that are separated by the calcium carbonate bands indicate a calm water environment in the flood basin area. The individual layers are suggestive of repeated flood events along a possibly sinuous stream during a humid climate when banks with strongly cohesive and constant sediment supply possibly meant restricted vegetation cover in the catchment. In between the episodes of overbank sedimentation there were probably periods of aridity, which facilitated calcium carbonate precipitation.

The soft sediment deformational structures within the fine-grained silty sand show fold structures of intra-formational character. These in some cases extend up to 15 m. The geometric shapes of these folds vary from wide open folds to flexures and monoclines. The calcrete bands show well developed plunging folds, where the fold axis trends towards south with a plunge of 10-15°. The wave length of the fold varies from 1.5 m to 2.0 m with an amplitude of 0.5 m. The monocline shows an apparent steepening towards west, suggesting that the down-faulted block lies to the west. The smaller, closely-spaced minor faults within the strata are significant indicators of syn-depositional tectonism. In another study by Jain et al (1998) at Rayka, four NW-striking faults were mapped, having throws ranging from 1 m to more than 3 m. They

related the growth of folds in synchronous sediment units. They showed that a slump sheet moved tens of meters northeastward down the  $0.7^\circ$  dip slope of one tilt block during displacement on its bounding faults.

The silty sand horizon is overlain by a highly mottled and pedogenised mud. This shows well-developed vertisol characters such as desiccation cracks, drab halos and calcium carbonate root casts. The deposit is typical of a flood plain and seems to have been deposited during the final phase of flood events in isolated flood pools. Intensive fracturing, reflecting pedogenic activity, has given rise to sub-angular aggregates described as peds. Peds form through repeated expansion and shrinkage of clays, coupled with root activity of plants. Striations formed due to preferential orientation of clay minerals are found on the ped faces. Calcium carbonate nodules and tubes occur throughout. Vertical fissures form in response to extreme drying events when the soil starts cracking. Greenish grey drab haloes consist of a white carbonate-rich core, enveloped by greenish grey clays, gradually merging with the host clays.

The vertisol is overlain by a 1-2 m thick Gravel-2 with trough cross-stratification. It occurs as isolated bodies dominated by poorly-sorted clasts of calcrete, quartzite and basalt. A wedge-like geometry is seen where stratification planes of the gravel extend into the adjacent sand unit to form a large trough. The lower bounding surface is erosive with respect to the underlying mottled clays. The fore sets show normal grading and dip of  $14^\circ$ - $25^\circ$  due SW to SSW in the northern sections and SSE, SSW and W in the southern sections (Malik et al., 1999). Trough cross-stratification is usually formed by the downstream migration of trains of sinuous-crested mega dunes in a deep channel profile. These troughs show decreasing amplitude towards the top, suggesting a declining flow. Such poorly-sorted, relatively large clasts ( $\sim 10$  cm) are indicative of enhancement in the flow intensity due to the change in the stream gradient. The trough axes of the fore sets are indicative of the channel orientation with high angle of plane beds ( $16^\circ$ - $18^\circ$ ), suggesting their deposition as point bars. Rolled carbonate nodules indicate the ability of the flow to erode the stable surface in the upper alluvial plain. The lithofacies are a product of sedimentation under a high flow regime in developing channel bars (Miall, 1978, 1985; Todd and Went, 1991). Overall, the evidence suggests the existence of an ephemeral fluvial system.

Gravel-2 is overlain by thick ( $\sim 10$  m) alluvium, comprising fine sand, silt and clay which is intercalated with three weathered horizons, identified as palaeosols (Fig. 9). These deposits form laterally-extensive sheets of silty sand with pedogenic calcium carbonate nodules, dispersed in sub-parallel layers. Higher silt content indicates their deposition away from the main channel as a floodplain deposit by a stream that

had a consistent flow path. The presence of palaeosols indicates the episodic nature of deposition with each phase of alleviation, followed by a period of pedogenesis. These possibly were caused by channel avulsion in association with continued aggradation after the deposition of Gravel-2. Alternately, these reflect episodes of climate-induced flow regime changes. The temporary hiatuses, corresponding to the pedogenesis, could be due to waning flow or channel avulsion. The three palaeosols show well-developed thick B horizon and complete absence of the A horizon. Each soil is somewhat different in colour. The lower and middle palaeosols are yellowish brown to grey in colour (10YR 5/4 and 10YR 7/4). Small sub-millimeter diameter buried root-channels, lined by carbonates, are seen. These soils generally are less calcified as compared to the overlying red (rubified) soil. Carbonate nodules occurring within the soil profile are orthic and irregular in morphology, and are on an average 1-2 cm in size. The granulometric analysis shows mean average grain size ranging between 3.33 and 3.96  $\phi$ . It comprises of an average 48-62% of sand, 28-36% of silt and 8-16% of clay, and is moderately well sorted. The clay mineral assemblage shows high concentration of montmorillonite with subordinate amount of kaolinite and illite. On the basis of granulometric analysis these soils can be categorized as sandy loam. The brown coloured horizons, which show higher concentration of clay as compared to the overlying rubified soil, suggest clay illuviation and soil formation, evidenced by the presence of root channels, development of aggregates (peds) and minor calcareous nodules. These features indicate that the soil is moderately developed. The presence of montmorillonite, along with subordinate kaolinite and illite, suggests a provenance similar to the red soil. The relatively higher content of kaolinite indicates a wetter climatic phase with an annual precipitation of more than 900 mm (Weaver, 1989). This clay mineral forms in high-leaching conditions. However, the presence of calcrete nodules (though less profuse) in these profiles is attributed to subsequent drier time spans.

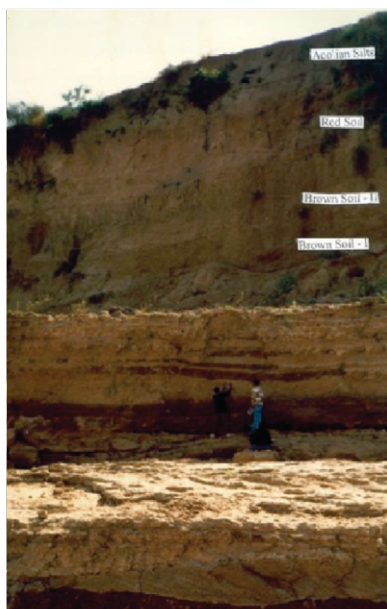
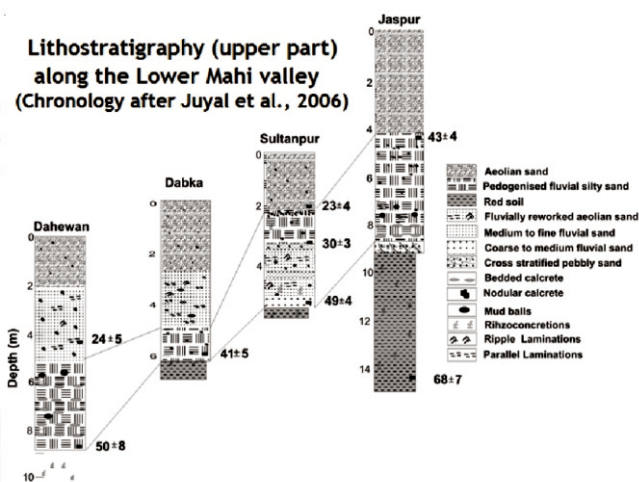


*Fig. 9.*  
*View of a cliff section showing sediment succession at Rayka.*

The upper soil, which has been used as a stratigraphic marker in the Mahi basin (Fig. 10), is yellowish red in colour (5YR 5/6). The granulometric analysis of this lithofacies shows mean grain size of 3.34-3.75  $\phi$ . The sediments are composed of 54-74% sand, 20-28% silt and 6-18% clay, and are moderately well sorted. The clay mineral assemblage is dominated by smectite (montmorillonite) with subordinate amount of illite and kaolinite. Hematite is observed in traces. On the basis of granulometric analysis this soil may be categorized as sandy loam. The undulating nature of the upper contact suggests a subdued palaeo-topography. Pedogenesis is indicated by clay concentration in the soil profile. The higher concentration of smectite (montmorillonite) along with subordinate amount of illite, kaolinite and hematite (in trace amounts) suggests that the clay minerals were derived from sediments containing ferromagnesian minerals, along with potash and sodic feldspars and micas (Weaver, 1989). This is also supported by the presence of basalt granules in the host sediments, the weathering of which led to the above mentioned newly formed clays, mainly smectite (montmorillonite). Presence of hematite in trace amounts may be because of lack of crystallinity of this mineral that was responsible for the coloration of the soil horizon (Pye, 1983). The carbonate nodules accumulated at the base of the soil profile forming a distinct zone, with sharp boundaries not connected to each other. These characters point to the nodules as being pedogenic calcretes, and their concentration in the lower part of the unit suggests that these were related to the weathering profile. The palaeo-precipitation values calculated using the equation given by Retallack et al. (1990) gives values of around 2000 mm for a depth of 350 cm. But as such values are unlikely for calcic soil, it is suggested that the red soil is actually a pedo-complex (cumulative soil) and spans a considerable period of time. The uppermost alluvial units are capped by fine aeolian sand and silt indicating the onset of aridity in the region (Fig. 10).



### Stop 2: Kothiyakhad Section

This section is located in the estuarine zone of Mahi basin. The S2 surface at Kothiyakhad occurs as a 3-6 m high, flat terrace and has been mapped all along the lower Mahi basin as an unpaired terrace (Maurya et al., 1997a, 2000), whose cliffy sections are cleaned by recent erosion (Fig. 11). Two major units identified in the successions are: (1) dark greyish brown clay with organic content and (2) greyish silty sand. These occur alternately with an erosional contact, and the base is unexposed. The clay units have yielded a good population of foraminiferids, whereas the silty-sand units have preserved fresh water ostracods. Radiocarbon dating of four organic-rich clay horizons at Kothiyakhad (Fig. 12) has provided dates of 3660±90, 3320±90, 2850±90 and 1760±80 yrs B.P. (Kusumgar et al., 1998). However, since the base of this sequence is not exposed, it is obvious that the actual deposition of the terrace sediments commenced prior to 3660±90 B.P. Radiocarbon dating of shells in the basal gravelly layer of a comparable fluvial terrace, overlying the basement rocks at



Fig. 11.

Cliff section of a valley fill terrace on estuarine sediments at Kothiyakhad, showing alternate dark clays and silty sand.

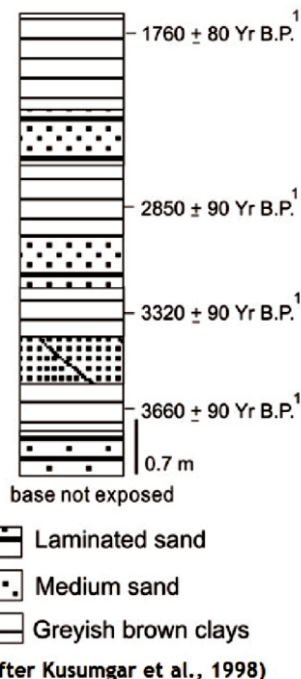


Fig. 12.

Litholog of the sediments exposed at Kothiyakhad with radiocarbon dates (after Kusumgar et al., 1998).

Vanoda in the pediment zone of Mahi River, has provided date of 6400±120 yr B.P. This suggests that the deposition of Holocene valley fill terraces was initiated within the river channels as the Holocene sea reached post-glacial high on the west coast at around 6000 B.P. (Maurya et al., 1997a, 2000; Hashimi et al., 1995). A total of 25 genera of foraminiferids were identified from the mud units of Kothiyakhad (Raj et al., 1998). Out of these, 23 are benthic comprising of *Brizalina*, *Bulimina*, *Bolivina*, *Biloculina*, *Lagena*, *Triloculina*, *Pseudobulimina*, *Hopkinsina*, *Sagrina*, *Ammonia*, *Cibicides*, *Discorbis*, *Discorbinella*, *Florilus*, *Hastegerina*, *Melonis*, *Nonion*, *Nonionella*, *Pyrgo*, *Pyrgoella*, *Pararotalia*, *Parafissurina*, *Rosalina* and few other Rotaliid. The two planktonic forms identified are *Globigerinoides sacculifer* (Brady), *Globigerina bulloides* (Parker, Jones and Brady), *Globigerina idesruber* (d'Orbigny). The silty-sand units have yielded 3 genera of ostracods, namely *Condonia*, *Darwinula* and *Ilyocypris*. Considering the morphology of benthic forms the 23 genera of foraminiferids were classified into two morpho-groups (Kusumgar et al., 1998): angular asymmetrical and rounded symmetrical.

In addition to the above, seismically-induced structures have also been observed in the Holocene terrace sediments at Kothiyakhad (Maurya et al., 1998, 2000). These include contorted laminations, load structures, convolutions, small-scale folds and syn-sedimentary micro-faults. Convolutions have been formed by tight folding of the beds, leading almost to the formation of pseudo-nodules. Downward-penetrating 'sand-dyke-like features' of fine sand into the underlying clay horizons is also observed due to seismic loading. The underlying horizons show effects of downward dragging, indicating that the dyke was forcibly intruded. Occurrence of load structures adjacent to these dykes and absence of any significant sediment cover suggest the role of seismic loading in the formation of these structures.

Soft-sediment deformational structures are important indicators of past seismic activity (Allen, 1975). The deformation took place due to liquefaction, which occurs during shaking of the sediments near the sediment-water interface, resulting in sagging or crumpling of the sediments (Maurya et al., 1998). Radiocarbon dating of organic-rich clay horizons (Kusumgar et al., 1998) from the Kothiyakhad section in the lower Mahi valley suggests that the deformation occurred during a late Holocene seismic event, which took place between 3320±90 and 2850±90 yrs. B.P. The Holocene tectonic activities thus played a role in the evolution of the Gujarat alluvial plains.

**Stop 3: Mujpur Section**

This section is located on the left bank of the Mahi River. The exposed succession is of about 6 m, showing alternate units of mud and silt. The base is not exposed and the 0.75-1.6 m thick laminated mud forms the base of the succession, which shows presence of sand lenses at places. The 0.75 m thick medium to fine grained sand that overlies this unit shows weak pedogenesis. This is overlain by 0.5 m thick horizontally-laminated mud. Alternating layers of silty-sand and mud of 1.2 m overlie it. The silty sand layer shows an average thickness of 20-30 cm, while the mud is 15-20 cm thick. This is overlain by 0.5 m thick laminated mud horizon, which is overlain by 1 m thick silty sand. Another 1 m thick laminated mud horizon overlies this silty sand. Finally, the succession is capped by a 0.5 m thick sand, showing well-developed soil unit. Soft-sediment deformational features can also be identified in Mujpur section (Maurya et al., 1998). These include injected liquefied sand, overturned folding, small-scale folds and syn-sedimentary micro-faults.

**Stop 4: Dabka Section**

This section is located in the present-day estuarine zone of the Mahi River. The cliff of 15 m is exposed on the left bank of the river, of which the basal 2 m succession is covered by scree material. The exposed succession shows well-developed 3 m thick medium to fine silty-sand horizon of red palaeosol (*Fig. 10*). The horizon is yellowish red (5YR 4/6) and is calcretised. The base of the horizon shows high concentration of calcrete nodule, ranging in size from 1.5 mm to 2.5 mm in diameter. The sediment size becomes coarser towards the top, along with the decreasing concentration of the calcrete nodules. In the upper part, the sediments are mainly silty-sand and show well-developed pedogenic features like buried rootlets, rhizo-concretions and burrows that are dark brown to black in colour. This is overlain by 5-6 m thick, horizontally-stratified silt horizon with sub-horizontal calcrete layers. The “loess-like” silts, which are 3 m thick, overlie this, and the succession is capped by 1 m thick dune sand (*Fig. 10*).

**Day 3: 14/11/2017****Vadodara to Gamod, Tilakwada, Chandod, Phulwadi and back  
Stay at Vadodara.**

Some of the highly interesting landscape features in Gujarat Alluvial Plains occur in the lower Narmada River basin. These will be visited to appreciate their geomorphological characteristics and evolutionary traits. To appreciate the landscape better, a short review of the Quaternary landscape development in the basin is provided below.

**Geomorphology and Late Quaternary Sequences of the Lower Narmada River Basin**

The Narmada River, the largest river of peninsular India, flows along the ENE-WSW trending Narmada-Son Fault (NSF), a well-known seismo-tectonic feature (Biswas, 1987). A major part of the course of the Narmada River falls within the rocky area comprising Late Cretaceous – Eocene basaltic lava flows, belonging to the Deccan Trap Formation. The river follows a constricted course in this reach, characterised by waterfalls, rapids, scablands and gorges (Rajaguru et al., 1995). The true alluvial reach of the Narmada is encountered in its lower part within the state of Gujarat. This reach is about 90 km in length and forms the southern margin of the N-S extending Gujarat Alluvial Plains. A significant feature of the lower Narmada valley is the deposition of a huge thickness of Tertiary and Quaternary sediments in a fault-controlled basin. To the south of the ENE-WSW trending Narmada–Son Fault (NSF), the Tertiary rocks and basaltic flows of Deccan Trap Formation occur on the surface, while to the north they lie in the subsurface and are overlain by Quaternary sediments. However, the overlying Quaternary sediments, having a maximum thickness of ~800 m (Maurya et al., 1995), still remain unclassified. Drill data from some of the deepest wells in the basin have revealed occurrence of Deccan Trap at depths of ~6000 m, followed by an Archaean basement (Roy, 1990). The Tertiary sediments, outcropping to the south of the NSF, represent the full sequence from Eocene to Pliocene, overlying the Deccan Trap, and show extensive deformation in the form of several ENE-WSW trending anticlinal highs and ENE-WSW and E-W trending reverse faults. Neotectonic studies along the NSF have been singularly lacking. However, some studies dealing mainly with the channel form, fluvial processes and hydrological aspects have been restricted to the middle and upper reaches of the Narmada River (Kale et al., 1994; Rajaguru et al., 1995; Gupta et al., 1999).

**Geological and tectonic setting:**

The Narmada River, the largest river of peninsular India, flows along the ENE-WSW trending Narmada-Son Fault (NSF), a well-known seismo-tectonic feature (Biswas, 1987). A major part of its course falls within the rocky area comprising Late

Cretaceous – Eocene basaltic lava flows which belong to the Deccan Trap Formation (Fig. 13). The river follows a constricted course in this reach, characterized by waterfalls, rapids, scablands and gorges (Rajaguru et al., 1995). The true alluvial reach of the Narmada is encountered in its lower part within the state of Gujarat. This reach is about 90 km long and forms the southern margin of the Gujarat Alluvial Plains. A significant feature of the lower Narmada valley is the deposition of a huge thickness of Tertiary and Quaternary sediments in a fault- controlled basin in the downthrown block to its north (Fig. 13). To the south of the ENE-WSW trending Narmada–Son Fault (NSF), the Tertiary rocks and basaltic flows of Deccan Trap Formation occur on the surface while to the north they lie in the subsurface and are overlain by Quaternary sediments. The Quaternary sediments, although having a maximum thickness of ~800 m (Maurya et al., 1995), still remain largely unclassified. Drill data from some of the deeper wells in the basin have revealed occurrence of Deccan Trap at a depth of ~6000 m, followed by an Archaean basement (Roy, 1990). The Tertiary sediments, outcropping to the south of the NSF, represent the full sequence from Eocene to Pliocene, overlying the Deccan Trap, and show extensive deformation in the form of several ENE-WSW trending anticlinal highs and ENE-WSW and E-W trending reverse faults (Fig. 13).

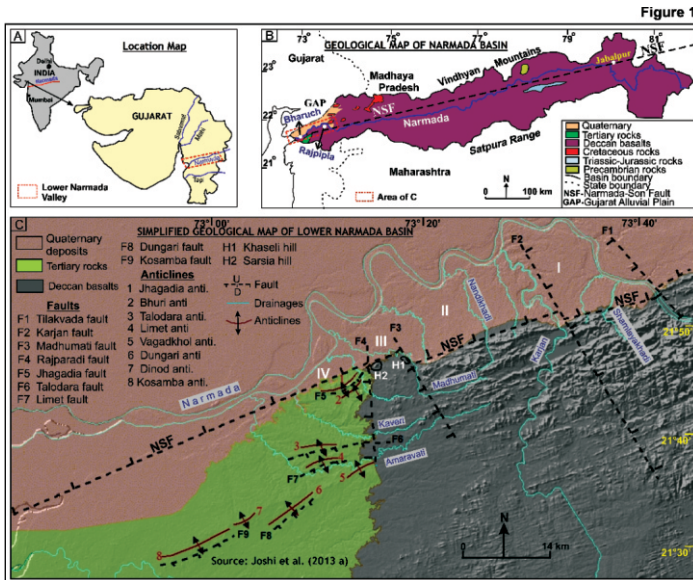


Fig. 13.

Location and geological setting of the lower Narmada river basin.

I to IV are the morphotectonic segments of the NSF (after Joshi et al., 2013a).

**Geomorphology:**

The lower Narmada valley can be divided into four broad geomorphic zones, spread across the four major morpho-tectonic segments. These are (1) an upland zone, dominantly on basaltic rocks but also on Cretaceous sandstones of Bagh Formation at places, (2) a lower highland on Tertiary rocks near the confluence with the sea, (3) a vast alluvial plain, which corresponds with the basin part, and (4) a narrow coastal zone dominated by mud flats (*Fig. 13*). Topographic profiles and field studies in the upland area reveal a rugged topography with steep escarpments bounding the mesa tops, flanked by deep and narrow gorges along the courses of several streams. Since the area consists mostly of south-dipping basaltic flows, the ridges and the associated intra-montane valleys trend in ENE-WSW direction (Joshi et al., 2013a). The lower highlands on the Tertiaries exhibit a hummocky topography in conformity with the anticlinal folds and faults. The straight ENE-WSW trending mountain-front scarps along the northern edge of the basaltic uplands and the along the lower Tertiary highland mark the NSF, beyond which lies the alluvial basin fill. The area is characterised by deep ravines, uplifted terraces, abandoned cliffs (palaeo-banks), incised cliffy banks and entrenched meanders (Chamyal et al., 2002; Joshi et al., 2013a). The alluvial plain between the ENE-WSW trending mountain-front scarps and the Narmada River has a gentle northward slope, while the plain to the north of Narmada River has a gentle slope towards WSW.

The geomorphic set up of the lower Narmada differs considerably from that in the middle and the upper reaches of the river, as described by Rajaguru et al. (1995) and Gupta et al. (1999). The river emerges from the Trappean uplands after crossing the NSF near Garudeshwar and follows a NW oriented fault-controlled course up to Tilakwada. The river then flows in a general WSW direction and exhibits large and deeply incised meanders. The Orsang, the Aswan, the Men and the Bhuki are the major rivers joining the Narmada from the north. The Karjan, which drains a major part of the trappean uplands in the lower Narmada valley, meets the Narmada from the south. The other tributary, the Madhumati River, drains the western fringe of the trappean upland. Between the Karjan and the Madhumati rivers there are several north-flowing small streams which meet the Narmada. The streams draining the lower highlands on the Tertiary rocks join the Narmada in the estuarine part, and their courses conform to the structural features in the Tertiary rocks.

The present drainage of the lower Narmada valley consists of deeply incised rivers, as evidenced by 40-50 m high alluvial cliffs and deeply entrenched meanders. Even the smallest streams, particularly those joining from the south, are found to have incised by 20-25 m. Presence of deep gullies (ravines), uplifted Holocene terraces, entrenched meanders and palaeo-banks, which comprise of abandoned, 15-30 m

high alluvial cliffs away from the present channel, suggest neotectonic activity in the area. The Narmada River exhibits characteristics of an underfit stream, characterized by narrow channels inside a wide belt of terraces (Dury, 1970). Even the largest seasonal floods do not overtop the cliffy banks (Gupta et al., 1999). Presently, the Narmada River has a tendency to shift towards the north (Agarwal, 1986). However, no traces of palaeochannels are found beyond the channel belt marked by a series of palaeo-banks. The meanders continue to grow towards the north, conforming with the northward shift of the river. Close examination of the palaeo-banks with the present channel confirms that the Narmada River has preferentially shifted towards the north. In the lower reaches the straight palaeo-bank coincides with the NSF, suggesting that the Narmada might have shifted away from the NSF due to neotectonic activity along this fault.

### **Geomorphic surfaces:**

Four major geomorphic surfaces have been mapped in the lower Narmada valley (Fig. 13). These are: (1) the alluvial plain ( $S_1$ ), (2) the extremely dissected ravine surface ( $S_2$ ), (3) a gravelly fan surface ( $S_3$ ), and (4) the flat-topped valley fill terrace ( $S_4$ ). The almost flat but gently-sloping alluvial plain, which occupies a major part of the area, has been designated as the  $S_1$  surface. This surface is extremely dissected in the vicinity of the river valley and exhibits gullies as deep as 20-30 m. We term this extensively gullied ravine surface as  $S_2$  to distinguish it from the un-dissected alluvial plain and the fundamental importance of the extensive dissection in the geomorphic evolution of the area. The  $S_3$  surface is a gravelly surface comprising a series of alluvial fans deposited along the mountain-front scarps of the NSF near Rajpipla. This fan surface is bounded by a NW-SE trending fault passing through the Narmada River on its eastern side and by a NNW-SSE trending fault passing through the Karjan River, a tributary of the Narmada, on its western side. The  $S_4$  surface is a wide flat-topped terrace surface of 5-12 m height, which occupies a deeply incised stream valley. The terraces show no evidence of ravine erosion and abut against the abandoned cliffs (palaeo-bank) of  $S_1$  and  $S_2$  surfaces.

### Lithostratigraphy and Sedimentation History

#### S<sub>1</sub> and S<sub>2</sub> surfaces:

The sediments that comprise the S<sub>1</sub> and S<sub>2</sub> surfaces are exposed along the 40-45 m high incised cliffs along the lower Narmada valley (Fig. 14). The sediment succession shows a basal clay, overlain by alluvial fan facies, and an alluvial plain facies dominated by overbank sediments (Fig. 14).

#### Basal clays:

The oldest deposit of the exposed sediment succession is a highly pedogenised mottled clay horizon, showing vertisol characters like extensive fractures giving rise to blocky aggregates, pseudo-anticlines and hydroplastic slickensides along the fracture surfaces. The deposit occurs at the base of the exposed sediment column (Fig. 14) and is readily identifiable owing to its laterally consistent occurrence and uniform lithology. Micro-faunal studies have yielded a rich assemblage of shallow marine foraminifers. The basal clays are overlain by thick fluvial sediments, which comprise two principal alluvial facies – the alluvial fan facies and the alluvial plain facies (Fig. 14).

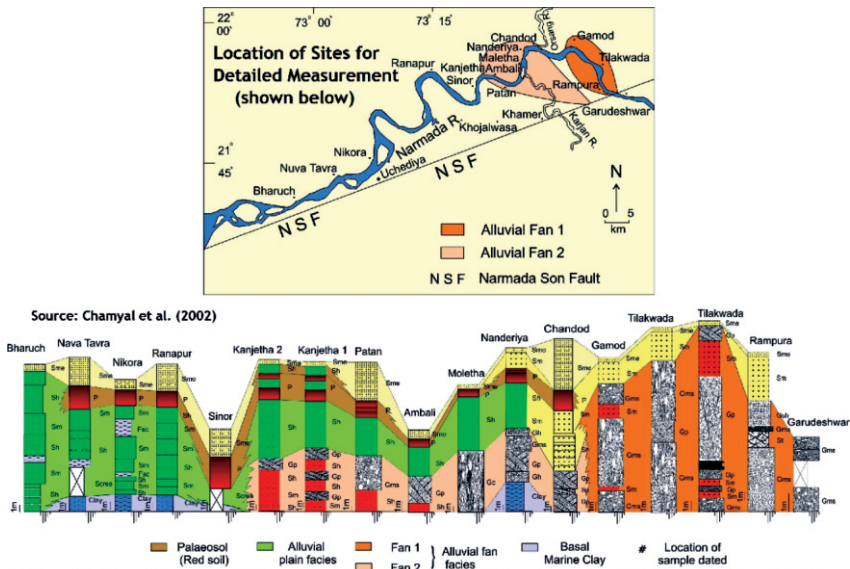


Fig. 14. Stratigraphy and lateral facies variation of Late Pleistocene sediments forming S<sub>1</sub> and S<sub>2</sub> surfaces in lower Narmada valley (after Chamyal et al., 2002).

**Fluvial sequence:**

The exposed sediments of the lower Narmada valley indicate two distinct phases of changes in the fluvial regime. One is the multi-distributary channel system that deposited the alluvial fan sediments (Chamyal et al., 1997, 2002), followed by finer alluvial plain sequence deposited by a large river in an alluvial plain setting. The reasons for the sudden change of multi-distributary river system to a more integrated single channel river system are not clear. The observed sedimentary characteristics of the alluvial plain sequence discussed above indicate a low sinuosity, single-channel large river that was hyper-avulsive. On a conservative estimate, the avulsions may have taken place on a scale of hundreds of years. The river was characterised by a ~ 8-15 m deep channel that was ~70-80 m wide, even during low discharge levels. Present-day large rivers show similar characteristics (e.g. Brahmaputra; Coleman, 1969) in which the sediments show large-scale bedforms while the river migrates at a high rate. Presently, the Narmada has a large drainage basin, much of which lies in the humid region further to the east of the Gujarat Alluvial Plain. This accounts for the high discharge levels of the Narmada River, which is next only to those of the Brahmaputra and the Ganga (Coleman, 1969).

The phase of alluviation up to the palaeosol appears to be synchronous regionally and globally. Studies in the adjacent river basins of the Mahi, the Orsang (Juyal et al., 2000; 2004) and the Sabarmati (Tandon et al., 1997) suggest a dominantly semiarid climate during large part of the Late Pleistocene and an ephemeral river system. Studies on the alluvial plain sedimentation in lower Narmada valley, however, indicates deposition by a large river which was sustained by a climate significantly wetter than at present. Although a general correlation of the depositional phases during Late Pleistocene is possible (Chamyal et al., 2002), the large-scale sedimentary bedforms of the type described here are not observed in the Mahi and the Sabarmati basins. The exposed sediments and the modern discharge levels of the Narmada River, therefore, present a contrasting picture as far as Gujarat Alluvial Plain is concerned.

The Narmada River in the Late Pleistocene has been inferred to be a mobile meandering river which carried large quantities of sand (Gupta et al., 1999), with periods of large floods (Kale et al., 2003). Studies on Holocene palaeo-flood deposits in central India (Kale, 1999; Kale et al., 1994; 2003; Ely et al., 1996) have revealed a strong correlation between periods of extreme discharges and stronger monsoons. We, therefore, infer that the alluvial plain sediments of the lower Narmada valley suggest humid climate in the large catchment area located further to the east. Additional evidence for a large catchment of the Narmada River during Late Pleistocene is provided by the dominance of sub-rounded clasts in the alluvial fan

sediments (Chamyal et al., 1997), which underlie the alluvial plain sediments. The sub-rounded clasts (a deviation from the normal angular clast composition of alluvial fans) has been attributed to longer distance of transport before they were deposited in an alluvial fan environment in the lower Narmada valley. This suggests that the Narmada River has maintained a large catchment at least during the last 100 ka. The alluvial plain sequence of the lower Narmada valley also suggests discharges higher than the present-day Narmada River in the upper part of the Late Pleistocene. The palaeosol near the top of the sequence, however, correlates with the regional phase of intense pedogenic activity in the Gujarat Alluvial Plain before the Last Glacial Maximum. The overlying stratified sands and silts reflect a significant weakening of fluvial regime during the arid phase of the Last Glacial Maximum, though the river still remained perennial, again mainly because of the large catchment area of the drainage basin.

Overall, the 50-25 ka period in north India is considered to be a period of widespread fluvial aggradation, as found from the studies on alluvial sequences in Gujarat Alluvial Plain (Tandon et al., 1997; Juyal et al., 2000; Maurya et al., 2000), Maharashtra upland rivers (Kale and Rajaguru, 1987), Central Narmada (Badam et al., 1986; Gupta et al., 1999; Kale et al., 2003), Son and Belan valleys (Williams and Clarke, 1984) and the Indo-Gangetic plain (Singh, 1996). Well dated global fluvial sediment records from Guadalope basin in Spain (Fuller et al., 1998), the entire Mediterranean region (Macklin et al., 2002), Thames River (Maddy et al., 2001), Mississippi River (Autin, 1996; Blum et al., 2000), and Australia (Nanson et al., 1992; Kershaw and Nanson, 1993) also suggest enhanced fluvial aggradation under a humid climate during the 50-30 ka period. There is thus a strong reason to believe that the deposition of alluvial plain sediments with large-scale bedforms below the palaeosol in the lower Narmada valley, was by a large river that operated in a more humid condition than at present, and possibly in response to global climatic perturbations. The humid climate, together with a large catchment area, contributed to high discharge, leading to the formation of large-scale sedimentary structures in these sediments.

## Geomorphic Evolution

### Late Pleistocene:

The sediments forming the  $S_1$  and  $S_2$  surface date back to Late Pleistocene. The sedimentation commenced with the deposition of the marine basal clays during the last interglacial high sea at  $\sim 125$  ka which is presumed to be about +7 m as revealed by the studies on the adjacent Mahi river basin (Rachna Raj et al., 1998) and Saurashtra coast (Pant and Juyal, 1993). Regression of this sea led to the initiation of fluvial sedimentation. The fluvial sediments indicate deposition in two fluvial macroenvironments— the alluvial fan environment and the alluvial plain environment. The alluvial fan deposits overlie the marine clays followed by the alluvial plain sediments.

Optimal conditions for fan development are created in regions undergoing extension (Blair and Bilodeau, 1988), like in the Basin and Range province of western North America, the Middle Eastern Dead Sea rift in the Middle East, and the East African rift system. Extensional basin settings are especially conducive for long-term fan development, leading to deposition of fan sequences hundreds of metres thick, but in a compressive tectonic regime the long-term development of fans is hindered due to the stronger component of lateral tectonic deformation (Blair and McPherson, 1994). The transformation of the Narmada-Son Fault (NSF) from a normal fault during the Tertiary to a reverse fault during the Quaternary is implicit in the seismic studies of the area (Roy, 1990). Additional evidence for prevalence of compressive stress regime in the lower Narmada basin is provided by numerous reverse faults in the Neogene sediments exposed immediately to the south of the Narmada-Son Fault (Agarwal, 1986). These evidences suggest that both the fans, Fan 1 and Fan 2, were formed in a compressive tectonic environment. This could be a reason why the maximum thickness of the fan sequences is about 70-80 m only, of which about 35 m is exposed. The compressive stress regime affected the fan morphology due to which both fans show a rather elongated shape, resulting in alluvial fans of unusual axial lengths (Chamyal et al., 1997). The alluvial fan sediments are overlain by a thick sequence of alluvial plain facies, which indicate termination of fan sedimentation and establishment of a more integrated drainage system.

Several studies document the effects of syn-sedimentary subsidence on the alluvial plain sedimentation (Shuster and Steidtmann, 1987; Brown and Plint, 1994; Kraus and Middleton, 1987; Kraus, 1992; Jordan, 1981; Hagen et al., 1985). Absence of soil profiles in the thick over-bank fines of the study area is indicative of syn-sedimentary subsidence of the basin. Soils can only develop on land surfaces which are relatively stable (Bull, 1991; Marriot and Wright, 1993). Since the facies associations contain no pervasive fining upward trends or lateral accretion features we assume that there

have been no major deviations in the mean flow directions. It is unlikely that a high-sinuosity channel will produce stacked system of fluvial deposits showing these characteristics (Shuster and Steidtmann, 1987). Strong similarity in the orientation of the deformation structures suggests subsidence in a thrusting environment along the NSF, which is consistent with the subsurface studies. A study by Shuster and Steidtmann (1987) in an area having almost similar structural setting as in the present study area, suggests that if and when subsidence rate is low, sand bodies with high degree of persistence and inter-connectivity can be expected, while if and when rapid subsidence takes place, such persistent sand bodies may not occur. We, therefore, infer that the deposition of these sediments took place when a low-sinuosity and relatively fixed river system existed in a slowly subsiding basin.

Syn-sedimentary subsidence of the basin due to differential movement along the NSF is indicated by the alluvial fan sediments, thick over-bank sediments and the deformation structures. Folding and faults with reverse movement in the over-bank sediments suggest a compressive stress regime along the NSF. This was followed by a brief period of tectonic stability, as suggested by the 4-5 m thick palaeosol (red soil) that can be correlated with the red soils exposed in the Mahi and Sabarmati River basins. A blanket of aeolian sediments over the fluvial sediments suggests a phase of widespread aridity that corresponded with the expansion of Thar Desert into the Gujarat Alluvial Plains (Allchin et al., 1978).

### **Early Holocene:**

Formation of extensive ravines and 45-50 m cliffs along the incised streams suggest that the ravine formation post-dated the aeolian sedimentation of Late Pleistocene period. Absence of ravines on the  $S_4$  surface consisting of mid-Late Holocene sediments, helps us to constrain the age of the ravine formation phase (and that of the cliff formation and stream incision) to the Early Holocene (~10 to 6 ka), which was a period of rapid sea level rise (Chappell and Shackleton, 1986; Hashimi et al., 1995). This means that the ravine formation and the stream incision were not related to the lowering of the sea level during the LGM. Had such fluvial activities taken place during the low sea level of LGM, one would have expected a much randomised distribution of aeolian sediments, preferentially within the gullies, but this was not so even in the Mahi and the Sabarmati basins where a more complete aeolian record has been found (Tandon et al., 1997; Juyal et al., 2000; Maurya et al., 2000). The aeolian sediments occur as a capping over the underlying fluvial sediments and are clearly along the incised cliff sections and in the ravines.

The above evidences suggest tectonic upliftment of the lower Narmada valley along the NSF during Early Holocene period. It resulted in the formation of extensive

ravines ( $S_2$  surface) and a deeply incised stream valley. The strongest supporting evidence for the Early Holocene tectonic uplift of the area comes from the sea level curves of the west coast of India which suggests a tectonic component of about 40 m at this time (Rao et al., 1996). Assumptions of increased precipitation during the Early Holocene humid phase can be discounted for following reasons: (1) the severe erosional phase occurred during a period of rapid sea level rise; (2) the sea level curves of the west coast of India indicate a strong tectonic component of about 40 m during Early Holocene; (3) the geomorphic evidences like consistent presence of >40 m high cliffs of Late Pleistocene sediments, deep gullies, entrenched meanders and anomalous NNW tilting of the  $S_1$  surface between Narmada River and the NSF; and (4) high precipitation of Early Holocene did not produce similar effects in more humid region like the Indo-Gangetic plain, a foreland basin to the south of the Himalayas. Even today, the Indo-Gangetic plain receives roughly three times more rainfall than the lower Narmada valley. The major rivers, the Ganga and the Yamuna having very high discharge in Indian subcontinent, should have produced identical geomorphic features of incised river valleys and extensive ravine erosion. Instead, these rivers exhibit extensive floodplains, large natural levees and back-swamps (Singh, 1996). That leaves tectonic uplift as the main cause for dissected  $S_2$  surface in lower Narmada basin. However, discharge level was perhaps much higher than at present, as indicated by the palaeo-banks consisting of Late Pleistocene sediments ( $S_1$  and  $S_2$  surfaces). The features suggest a much wider and less sinuous channel belt for the Narmada River during the period. Even the largest seasonal floods are not enough to fill the entire present-day valley (Gupta et al., 1999).

As a preliminary conservative estimate, not considering the likely cliffy section below the exposed base, an uplift of about 40 m can be inferred from the 40-45 m high incised cliffs. This means that the 35-40 m high precipitous cliffs along the river actually led to an underestimation of the total amount of incision prior to the Mid-Late Holocene aggradation. The tectonic uplift during Early Holocene perhaps suggests inversion of an earlier subsiding basin. Such inversions of the basin have been common during the Tertiary period, and are well recorded in the sediments of this age (Roy, 1990).

The displaced Late Pleistocene sediments across NSF in the Narmada and the Karjan river valleys, the NNW tilting of the  $S_1$  surface consisting of Late Pleistocene sequence, anomalous topographic slope in the same direction, and incised cliffs up to 20-30 m in the streams that flow along this slope in the area between NSF and the Narmada River, indicate a differential uplift along the NSF during Early Holocene. The displacement of sediments of the  $S_1$  surface across the NSF indicates differential movement of about 35 m along the NSF during Early Holocene. The block between

the Narmada and the Karjan rivers, bounded by the NSF and the two other cross-faults, suffered subsidence leading to the formation of a series of alluvial fans over the Late Pleistocene sediments. The 5-8 m incised cliffs of the streams also suggest that this block escaped the uplift-induced large scale incision and ravine erosion that were going on simultaneously in other areas of the lower Narmada valley.

### **Middle Holocene to Recent:**

The Mid-Late Holocene valley complex is the product of a Holocene high-sea-level-induced deposition in a deeply incised fluvial valley. The Mid-Late transgression was within the incised fluvial valley, which resulted in estuarine sedimentation in the lower reaches and fluvial deposition in the upper reaches. A significant slowing down of the tectonic uplift facilitated the encroachment of the sea into the valley and creation of a depositional wedge, which extended up to the foothills. The 5-10 m exposed thickness of the valley fill sediments reveal tide-dominated estuarine deposition in the lower reaches and fluvial deposition upstream of the tidal reach. Seismically-induced soft sediment deformation features from comparable terrace sediments in the Mahi valley (Maurya et al., 1998) and the Orsang valley (Maurya et al., 2000) suggest tectonic instability of the region during the period of valley fill sedimentation. Comparison of the present estuary with the one indicated by the palaeo-banks against which the terraces abut, reveals that the present mouth of the Narmada River has roughly retained the original funnel shape of the estuary formed during the Mid-Late Holocene. However, the size of the estuary is now considerably reduced. The present estuarine reach contains several islands, which are coeval with the terrace surface and are well above the present tidal range. Hence, they are the products of estuarine processes of the Mid-Late Holocene and not those of the present day. Funnel-shaped morphology and increasing tidal energy landward are characteristics of tide-dominated estuaries (Wright et al., 1973).

Existing data suggest that the Mid-Late Holocene sea level has remained almost at the same level up to the present with minor fluctuations (Chappell and Shackleton, 1986; Hashimi et al., 1995). The Mid-Late Holocene sediments show tilting of 10°-20°, which is more pronounced in the vicinity of the NSF, suggesting that the incision and upliftment of the valley fill terraces well above the present day tidal limits is related to the continued differential uplift along the NSF. Evidence of tectonic uplift from the coast is also reported in the form of raised mudflats at 2-4 m above the present sea level (Merh, 1993). Currently, the river occupies the northern margin of the Early Holocene channel belt and is clearly more sinuous. It exhibits a narrow channel with wide meanders in between a set of Mid-Late Holocene terraces (S<sub>4</sub> surface), a typical pattern of under-fit streams (Dury, 1970).

Neotectonic studies are mainly based on geomorphic data associated with active faults, as well as on deformation structures. The geomorphic evidences observed in the lower Narmada valley are the young mountain-front scarps delimiting the basaltic uplands and marking the Narmada-Son Fault, youthful channel morphology of the Narmada River and other rivers, as testified by consistent presence of incised vertical cliffs, entrenched meanders, extensive and deep ravines, uplifted Holocene terraces, anomalous slope variation of  $S_1$  surface, especially to the south of the Narmada River, and remarkable correlation of the drainage with structural features in the lower uplands on the Tertiary. Two major phases of tectonic activity along the NSF are recorded. The first phase includes the Late Pleistocene when slow syn-sedimentary subsidence of the basin took place along the NSF, which allowed for uninterrupted sedimentation except for brief periods of pedogenesis of basal clays and the over-bank sediments. Syn-sedimentary subsidence of the basin in compressive tectonic setting is evidenced by the hindered alluvial fan sedimentation, thick over-bank sediments and associated sediment deformation. The second phase includes the Holocene, which is marked by basin inversion due to differential uplift along the NSF. Inversion of basin after a prolonged period of subsidence is common (Ziegler, 1983). The period of inversion is usually a period of net erosion (Mather, 1993). As stated above, two phases of uplift during Holocene could be recognised. The first of these occurred during Early Holocene which formed extensive ravines and a deeply incised fluvial valley. The second during Late Holocene to Recent uplifted the Mid-Late Holocene sediments forming terraces.

The Early Holocene tectonic activity recorded in the lower Narmada valley, possibly, has wider ramifications when viewed in the larger perspective of Indian plate. Available models of neotectonic deformation of the Indian plate indicate that the peninsular India has been undergoing high compressive stresses due to the sea floor spreading in the Indian Ocean and locking up of the Indian plate with the Eurasian plate in the north (Subramanya, 1996). Much of these N-S directed stresses have been accommodated by the under-thrusting of the Indian plate below the Eurasian plate. A part of these compressive stresses are accumulated along the NSF, a major E-W trending crustal discontinuity in the central part of the Indian plate. Tectonic activity of significant magnitude during the Early Holocene has been reported from the sea level studies of the west coast and from the Himalayas, located at the trailing and leading edges of the Indian plate, respectively. In the Himalayas, the termination of lacustrine sedimentation has been attributed to tectonic activity during the Early Holocene (Kotlia et al., 2000). Together, the evidences suggest a renewed phase of extreme compression of the Indian plate, which led to tectonic inversion along the NSF in the lower Narmada valley. Significant increase in compressive stresses accumulating on an intra-crustal fault like the NSF can transform a previously

subsiding basin into an uplifting one. Since the NSF has been characterised by compressive stress regime throughout the Quaternary, we believe that such variations in the degree of compression, which can in turn be interpreted in terms of varying rates of plate movement, alone are responsible for the Late Pleistocene subsidence and Holocene tectonic inversion in the lower Narmada valley. Studies from other parts of the NSF are needed to confirm the continuity of these movements along the length of the fault.

As stated earlier, the present landscape of the lower Narmada valley comprises of four geomorphic surfaces, which have evolved mainly due to tectonic activities along the NSF in a compressive stress regime. The sediments comprising the  $S_1$  and the  $S_2$  surfaces were deposited in a slowly subsiding basin during the Late Pleistocene. The Holocene period is marked by the inversion, which had earlier suffered subsidence. The inversion of the basin is due to significant increase in the compressive stresses along the NSF during Early Holocene, resulting in differential uplift of the lower Narmada valley. The continuation of the compressive stress regime due to the ongoing northward movement of the Indian plate indicates that the NSF is a major candidate for future intra-plate seismicity in the region.

The alluvial plain sequence of the lower Narmada valley is characterised by the dominance of over-bank sediments and large-scale sandy bedforms. The sequence was deposited by a low-sinuosity large river with discharge higher than during the present. The river migrated laterally across the alluvial plain at a high rate. The deposition was mainly controlled by the humid conditions prevailing in the large upstream catchment area further to the east of the present study area, and not by the semi-arid climate of the Gujarat Alluvial Plain. Studies so far suggest that the Narmada River has retained a large catchment since the last 100 ka.

### Stop 1: Gamod Section

Along the banks of the river Aswan the 15 m thick succession of Gms facies is characterized by convex upward surfaces. A major bounding surface separates two vertically stacked packages, each containing four cycles of the Gms facies (Chamyal et al., 1997). At the base of the succession is a sand sheet deposit (Sm facies), which separates the underlying sheet of the Gms facies from the eight cycles of debris flows. The dominant clast size is 10 cm. Deviation from this size occurs in the form of ~16 cm tabular blocky clasts. No St and Gp facies are observed at this locality.

### Stop 2: Tilakwada Section

The sediments of Alluvial Fan-1 are best exposed at Tilakwada, where the fan deposit occurs all along the cliffy banks of the Narmada (*Fig. 15, 16*). The section illustrates various characteristics of facies development, both spatially and temporally (Chamyal et al., 1997).

The sedimentary facies at Tilakwada section typically point to deposition in an alluvial fan environment (*Table 1*). The 30 m thick bank scarps expose a succession of a ubiquitous packet of Gms facies. The facies is present at the base of all exposures in the area. These gravels have lobate geometries, contained within which are lenses of the Gp facies. The clasts have thin white veneers of calcite,



*Fig. 15.*

*An incised cliff section at Tilakwada, showing the alluvial fan sediment succession.*



*Fig. 16.*

*Deeply incised right bank cliff at Tilakwada showing alluvial fan sediments.*

which has also cemented the gravel. The clasts are basaltic and some show remnants of pre-depositional spheroidal weathering. Nesting of clasts is present. The Gp1 facies occurs intercalated between Gms gravels, and progressively

becomes more prominent towards the top of the section. The alluvial architecture, when traced over long exposures using panoramic photographs, reveals the major contribution of the Gms facies. The oldest exposed sediments at Tilakwada are made up of 2 m thick, matrix-supported gravels. At places the thickness is about 6.5 m. The clasts range in size from 25 to 35 cm, and are dominantly basaltic. These are bounded together by a sand matrix. The top of the sediment succession is represented by a massive sand of about 2.5 m thickness, showing no internal stratification. This internally unstratified horizon was dated by Blue Green Stimulated Luminescence (BGSL) technique at PRL, Ahmedabad, and is found to be <90 ka in age (Chamyal et al., 2002). Over the massive sand deposit lies a planar, cross-stratified gravel bed having a thickness of about 5 m. At places it alternates with the massive sand horizon.

The alluvial architecture was constructed by both the confined and the unconfined flows. Of the primary depositional processes that directly contributed to aggradation of the fan, viscous debris-flows played a major role, with a minor contribution by sheet-floods. Debris-flow deposits (Gms facies) make up over 70% of the alluvial architecture. Debris-flows aggraded the fan at both proximal and distal ends. The maximum clast size decreases progressively down-fan, in agreement with the expected fall in flood velocity. Evidence of intervening quiescent periods between the fan aggradation events is present in the form of large-scale planar cross-stratified gravel (Gpt) and trough cross-stratified sand (St) facies. Braided rivers with longitudinal gravel bars dominated the surface of the fan during these phases. A major deviation from the norm is observed in the clast roundness of the debris-flow deposits. Most of alluvial-fan deposits are recognized by their angular to sub-angular nature. Angularity of clasts has been stressed and the only exception accommodated is a conglomeratic provenance. In the present case it is suggested that the greatly elongated catchment area upstream of Nawagam (fan apex) was a determinant. Rounding of clasts took place when the angular fragments were transported as bed load along the length of the Narmada. The flat base suggests that these clasts rested on a stream bed while the exposed surface of the clast was modified to its present shape by the stream flow. These sub-rounded clasts were then eroded from the bars, remobilized and entrained in viscous debris-flows during flash floods.

*Table 1. Summary of major sedimentary facies comprising the alluvial fan sediment succession at Tilakwada. Facies coding scheme is after Miall (1985).*

Facies Code	Description	Interpretation
Gms	Inversely graded cobbly to boulder gravels, having cross-sectional lobate geometry. Maximum clast size is up to 150 cm. Large clasts within each unit appear to 'float'. Clasts are usually sub-rounded basalts.	Debris flow deposits
Gms	Gravel-sand couplets, stratified, but no internal stratification. Sandy units contain pebbles but cobbles are absent. Clasts are usually sub-rounded basalts.	Sheet flow deposits
Sm	Sand sheets, massive with lobate flow deposits cross-sectional geometry, no visible internal stratification.39.1	Sheet flow deposits
GPI	Planar cross-stratified gravel; may occur as solitary set or co-set; show normal grading with clasts of sub-rounded basalt. At times cobbly basalt lag deposits are present.	Longitudinal gravel bars
Gp2	Planar cross-stratified gravel with lensoid geometry. Normally graded; intimately associated with Gms facies	Re-channelized flows genetically related to debris flow events
St	Trough cross-stratified sand.	Channel-fill element

### Stop 3: Chandod Section

The 35 m thick fluvial sediment succession exposed at Chandod (*Fig. 17, 18*) has been considered as the basis for the reconstruction of physical stratigraphy of the alluvial plain sediments above the alluvial fan sequence (Bhandari et al., 2005). The base of the section is characterized by a 3 m thick planar cross-stratified gravel (size ranging from 10-15 cm) and the matrix holding the gravels is sandy. These are overlain by 2 m thick planar cross-stratified sand, which is overlain by planar cross-stratified gravels having a thickness of 4 m.

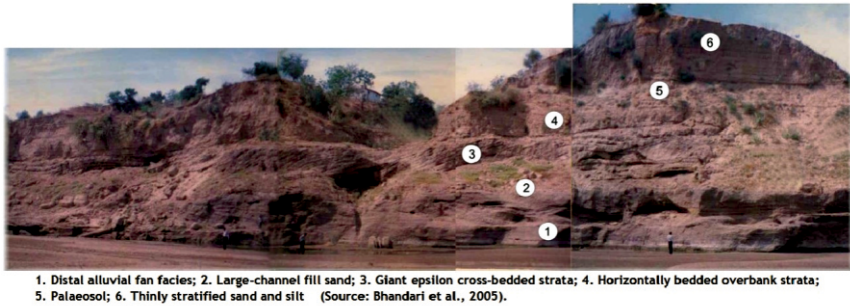


*Fig. 17.*

*Photomosaic of an extensive cliff at Chandod.*

*All units show erosional bases (after Bhandari et al. 2005).*

- 1) distal alluvial fan facies, 2) large channel fill sands,  
3) giant epsilon cross bedded strata, 4) horizontally stratified overbank strata,  
5) palaeosol, 6) thinly stratified sands and silts.*

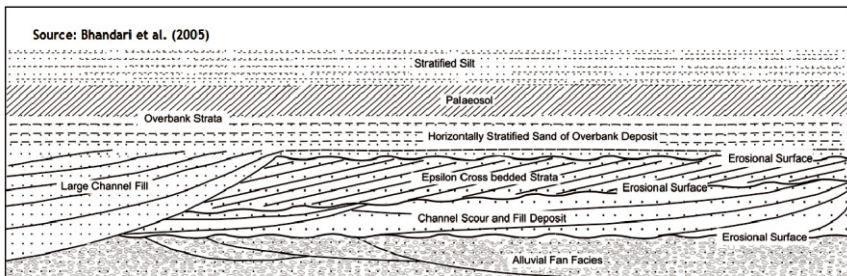


*Fig. 18.*

*Sketch showing vertical relationship between sediments exposed along the > 400 m long cliff at Chandod, as shown in Fig. 17 (Bhandari et al. 2005).*

Above the planar cross-stratified gravels a 10-m thick horizontally stratified sand is deposited. This sand horizon is studded with rhizo-concretions and horizontally-stratified bedded calcretes. These are overlain by a 5-m thick sand showing no internal stratification, which is again overlain by pedogenized sand of about 5 m thickness. A soil has developed over the fluvial over-bank fine sand and silt, and shows typical fracturing in the form of blocky aggregates. There is copious amount of calcrete throughout the horizon. The soil shows typical reddish brown colour. Overlying this is 6 m thick deposit of massive sand which shows no internal stratification.

At two stratigraphic levels channel fills are observed, which are separated by the epsilon cross-stratified facies (*Fig. 17, 18*). The older channel fill overlies gravel deposits of the alluvial fan facies with a deeply scoured base, and shows a gentle concave geometry, filled by vertically-accreted fine to medium sand. Overall, the structure indicates a westward-oriented channel that was ~70 m wide and ~4 m deep. Each sheet of channel fill is about 1 m thick and the channel axis decreases at the margins to 0.3 m. The sand shows fine horizontal laminations and a complete absence of lateral accretion feature. This suggests filling up of the channel primarily through vertical accretion in an almost standing body of water. It normally happens in chute cut-offs where deposition takes place in the remaining body of standing water after the channel is abandoned. The channel margins show a low dip of 15-20°, which means that the channel was not produced by incision. The younger channel fill is exposed at the southern extremity of the ~400 m long outcrop. Its shape suggests a much deeper and larger channel although only about 30% of the total structure is observed, the rest having been eroded away by the present river. The channel fill occurs above the epsilon cross-bedded strata. Its margin has a steep dip of about 30°. Extrapolation of the channel margin suggests a ~80-90 m wide and ~10 m deep channel. The channel trough is filled by sand sheets with concave-up geometry with internal stratification. Laterally sediments of this channel fill are found to grade into stratified over-bank sand. The epsilon cross-strata at Chandod range in thickness from 10 m to 15 m, and terminate against the overlying thick-bedded over-bank facies. Laterally, the epsilon bed passes into horizontal strata, and further away merges with the over-bank deposits. Its deposition can be attributed to lateral migration of a 15-20 m deep sand-bed stream. Similar large-scale epsilon cross bedded strata has been attributed by Jackson (1978) to deposition in deep water.

#### Stop 4: Phulwadi Section

This section on the right bank of Shamariyakhadi River exposes alluvial fan sediments forming the S4 surface in front of the NSF scarps (Fig. 19, 20). The alluvial fan is one of the five small coalesced alluvial fans recognized along the NSF scarps to the east of Rajpipla. The fans form a distinct northward sloping alluvial surface. The exposed sediments along the river cliff represent sediments of the medial part of the fan. The sediments are made up of matrix-supported gravels, horizontally-stratified gravels, planar cross-stratified gravels and sand (Fig. 20).

The gravels are sub-angular to sub-rounded, and are poorly sorted. Four aggradational phases of Gms facies are recognized. Sp and Sh facies occur as lenses or as continuous bands. The Sp, Sh and Sm facies represent the quiescent periods between the fan aggradation events. Overall, the section shows domination of Gms facies, and indicates cyclic aggradation phases. This suggests deposition mainly by debris flows and sheet flows.



Fig. 19.  
Upstream view of the incised cliff at Phulwadi showing early Holocene fan deposits with distinct layers of matrix-supported gravels and horizontally-stratified sand.

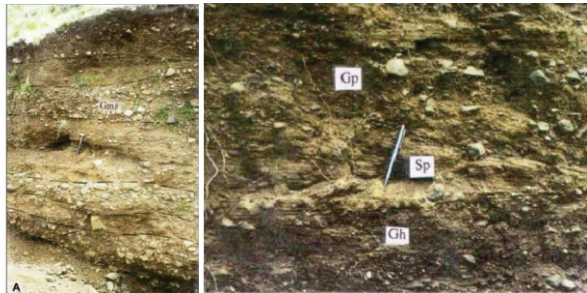


Fig. 20.  
(A) Four aggradation phases of Gms facies with intervening Sh facies at Phulwadi.  
(B) Lensoid nature of Sp facies overlain by Gp facies and underlain by Gh facies.

**Day 4: 15/11/2017****Vadodara to Juna Ghanta and Nava Ghanta along the Nandikhadi River, Khojalwasa, Tejpur, Karjan Dam, and back****Stay at Vadodara.**

The lower Narmada basin exposes some good examples of tectonic landforms and structural features along the Narmada – Son Fault, which are proposed to be visited during the day. Before describing the sites we provide a brief account of the tectonic geomorphology of the fault zone.

**Tectonic Geomorphology of the Narmada-Son Fault Zone****The Narmada-Son Fault:**

The Narmada–Son Fault (NSF) trends in ENE-WSW direction and is laterally traceable for more than 1000 kms. It divides the Indian plate into two geologically distinct provinces: the Vindhyan-Bundelkhand province to the north and the Deccan province to the south, and has a long tectonic history dating back to the Archaean times (Ravi Shankar, 1991). According to Ravi Shankar (1991) NSF is part of a large, composite, tectonically-controlled zone through the middle of the Indian plate, which can be termed as 'SONATA' zone (abbreviated form of the Son-Narmada-Tapti Lineament zone). The Narmada and Tapti Rivers follow these tectonic trends all throughout their course. Other synonyms used to describe this zone include the Narmada-Son Lineament (NSL; Choubey, 1971), Central Indian Shear (CIS; Jain et al., 1995) and Central Indian Tectonic Zone (CITZ; Radhakrishna and Ramakrishnan, 1988; Acharyya and Roy, 2000). Geophysical studies in the central part of this zone reveal this to be a zone of intense deep-seated faulting (Reddy et al., 1995). The zone witnessed large-scale tectono-thermal events associated with huge granitic intrusions around 2.5-2.2 Ga and 1.5-0.9 Ga (Acharyya and Roy, 2000). It was again reactivated during the Deccan volcanic eruptions during Late Cretaceous-Palaeocene periods (Agarwal et al., 1995). Profuse occurrence of E-W trending dykes suggests that the zone formed the main centre of eruptive activity (Bhattacharji et al., 1996). The entire zone is presently characterized by high gravity anomalies, high temperature gradient, heat flow and anomalous geothermal regime (Ravi Shankar, 1991), which suggest that the zone is thermo-mechanically and seismically vulnerable in the framework of contemporary tectonism (Bhattacharji et al., 1996).

Data on the NSF in this part is mainly the result of extensive geophysical surveys for exploration of petroleum reserve. The westward extension of the NSF zone into the lower Narmada valley exhibits itself as a less complex structural setting, and expressed as a single deep-seated fault (NSF) that has been confirmed by the Deep Seismic Sounding studies (Kaila et al., 1981). Seismic reflection studies have established that the NSF is a normal fault in the subsurface and becomes markedly

reverse near the surface (Roy, 1990). Reactivation of the fault during the Late Cretaceous led to the formation of a depositional basin in which marine Bagh beds were deposited (Biswas, 1987). The NSF remained tectonically active since then, with continuous subsidence of the northern block, designated as the Broach block, which accommodated 6-7 km thick Cenozoic sediments (Biswas, 1987). The total displacement along the NSF exceeds one kilometre within the Cenozoic section (Roy, 1990). However, the movements along this fault have not been unidirectional throughout. The general tendency of the basin to subside has been punctuated by phases of structural and tectonic inversion (Roy, 1990). The N-S directed compressive stresses during the Early Quaternary folded the Tertiary sediments into a broad syncline, the Broach syncline, in the rapidly subsiding northern block (Roy, 1990). The Broach syncline extends from the NSF to the Mahi River in the north. The E-W trending axis of this syncline lies to the north of the Narmada River. Corresponding anticlinal structures are found in the Tertiary rocks exposed in the southern up-thrown block. Historical and instrumental records indicate that the compressive stresses still continue to accumulate along the NSF due to continued northward movement of the Indian plate. This is evidenced by the fault solution studies of the earthquakes at Broach (23rd March, 1970) and Jabalpur (22nd May, 1997), which suggest a thrusting movement (Gupta et al., 1972; 1997; Chandra, 1977; Acharyya et al., 1998).

### **Stop 1: Traverse along the Nandikhadi River through Juna Ghanta and Nava Ghanta**

The Nandikhadi River is a tributary of the Narmada River, and originates in the south from the Trappean uplands. It is the most important drainage basin to the south of the Narmada River as it shows significant evidence of active tectonics (*Fig. 21*). In the upland zone, the Nandikhadi River is characterized by frequent occurrence of knick points, tight meanders and deeply incised channel segments (*Fig. 21*). The height of the knick points ranges from 1 m to 16 m. The total fall of gradient related to knick points is of ~37 m within a short distance of 1.5 km.

A coalesced group of alluvial fans, the 'bajada', is identified in this segment between the Karjan River and the Madhumati River (Joshi et al., 2013b). The sediments are well-exposed along the Nandikhadi River and shows a higher topographic elevation compared to those in the adjacent alluvial plains to the east of Karjan valley, to the west of Madhumati valley and the Narmada valley to the north. The altitude of the fan surface near the mountain front is 120 m above msl and it extends for ~24 km along the mountain front.



Fig. 21.

*Geomorphic set up of Nandikhadi river basin (after Joshi et al., 2013a). (A) Sharp physiographic contrast along the NSF and the deeply incised Nandikhadi River channel (view looking south). The scarps expose south-dipping basaltic flows of the Deccan Trap Formation. Arrows indicate downstream direction of the river. (B) A ~10 m high waterfall along the Nandikhadi River near the upland zone. Note the upstream dipping basaltic flows. (C) Slickensided surface of the transverse Madhumati Fault in basalt at Tejpur, indicating oblique slip movement.*

As the river course approaches the unconsolidated Quaternary sediments, it shows incision of up to 40 m, which decreases to 6-7 m in a very short distance of less than 3 km. The bajada sediments can be inspected along the cliffs exposed along the incised river. In longitudinal section, the deposits appear to be wedge-shaped (Fig. 22). The bajada surface displays plano-concave-upward geometry, created by the distally decreasing slope. The sediments can be grouped under seven distinct sedimentary facies. In approximate order of abundance, the facies identified are: matrix-supported gravel (Gmm), clast-supported gravel (Gcm), massive silty sand (Sm), soil (P), trough cross-bedded gravel (Gt), horizontally-stratified gravel (Gh), and massive brick-red sand (Ss) lithofacies. The OSL age of 25.1±1.8 ka BP obtained from the middle part of the bajada succession suggests that the sedimentation occurred during the later part of late Pleistocene. This correlates with the slow syndimentary subsidence of the basin during the late Pleistocene, as documented by Chamyal et al. (2002). Compared to this, the late Pleistocene sediments exposed along the incised cliffs of Narmada River are finer as they were deposited in an alluvial plain environment (Bhandari et al., 2005). The bajada sediments are sedimentologically different but stratigraphically comparable with the sediments

exposed along the Narmada River. It is presumed that in the downstream, the bajada sediments may show inter-tonguing relationship with the finer alluvial plain sediments of the Narmada River.

The Quaternary sediments occur at an altitude of ~120 m above msl and represent the sediments of proximal fan deposits. The succession starts with deposition of clast-supported massive gravels (Gc) that directly overlie the Deccan Trap with an abrupt contact. It consists of sub-angular to sub-rounded clasts of Deccan basalt and range in size from pebble to boulder. There is a general absence of grading despite the massive thickness, which suggests that the clast-supported gravels were deposited by low strength, pseudo-plastic debris flows. The clast-supported gravels are overlain by massive silty sand (Sm) and horizontally-stratified gravel deposits (Gh). The downstream sediment succession represents distal part of the fan comprising of soil, horizontally stratified gravels and massive silty sand (Fig. 22).

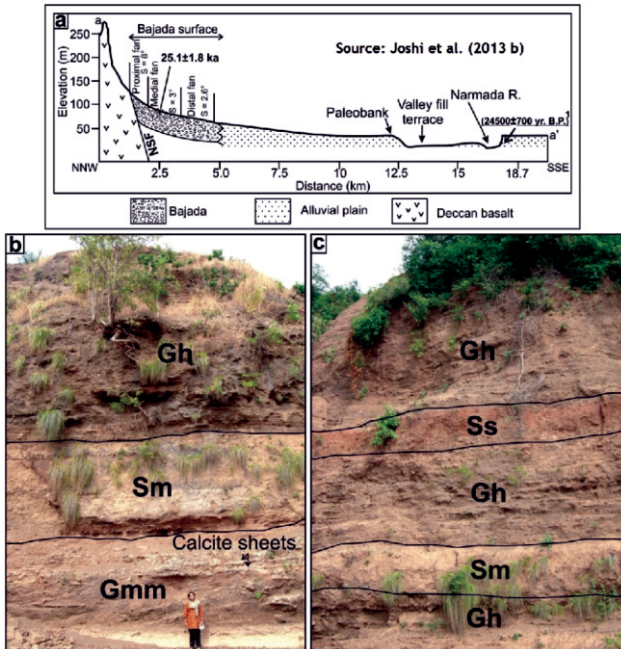


Fig. 22.

(A) Topographic cross profile of the bajada surface drawn from DEM. Note the wedge shaped coarse gravelly bajada sediments in front of the hill and their mean slope. Other surfaces down the slope are also shown (after Joshi et al., 2013b). (B) and (C) are field view of the cliff exposing bajada sediments.

### Stop 2: Khojalwasa Section

The bajada sediment succession at this site represents distal part of the fan, comprised of soil, clast-supported gravels, horizontally-stratified gravels and massive silty sand (Joshi et al., 2013a). A brownish to reddish soil corresponds to lithofacies P of Miall (1996). Parent material of the soil is a mixture of clay, silt and fine sand. Hence it can be inferred that it was possibly deposited by the stream as over-bank deposits. The presence of soil suggests a sub-humid climate or a relatively wetter climate than at present. The clast-supported massive gravels correspond to the Gcm facies of Miall (1996). It consists of sub-angular to sub-rounded clasts of basalt and range in size from pebble to boulder. The massive silty sand facies (Sm) is characterized by 0.25 to 4.5 m thick horizons of fine to medium sand and silt. The sand is poorly sorted and do not show any grading. It is rich in calcium carbonate nodules and calcite sheets. The absence of sedimentary structures, massive texture and poorly sorted framework suggest that the lithofacies was deposited as sheet flood deposits by gravity flows. The horizontally stratified gravel (Gh) is the most abundant facies, deposited particularly in the proximal and medial sectors of the fan surface. The thickness of the facies varies from 5 m to 17 m. It has a clast framework and abundant coarse sandy matrix. However, the percentage of matrix varies considerably. The Gh facies represents the longitudinal bar deposits of braided channels.

### Stop 3: Tejpur in Madhumati River basin

The Madhumati River is one of the major tributaries of the Narmada River, joining from the south. The river rises from the Trappean upland, drains the western fringe of the Trappean upland, and traverses through the NSF and alluvial plain to join the Narmada after a travel length of about 41 Km. The drainage characteristics within the Trappean uplands and in the alluvial zone are quite different. While in the upper reaches of the river through the Trappean zone the drainage pattern is trellis, in the lower reaches through the alluvium the pattern is dendritic. Stream density in the upper reaches is high, where the tributaries are straight, whereas in the lower reaches the stream density is low, and tight entrenched meanders can be observed. The drainage basin is elongated in NE-SW direction. The course of the Madhumati River shows a strong structural control. From Umarkharda to Dholi the river flows westward along an almost E-W trending course. At Dholi, the river takes a right angle turn to flow northward along a remarkably straight N-S oriented course up to Tejpur which lies to the north of the NSF. The straight nature of the river course and the right turn strongly suggests the existence of a N-S trending transverse fault (Fig. 23). The geomorphic evidence of the NNW–SSE trending Madhumati Fault is observed near Tejpur. The fault is represented by the displaced scarps of the NSF, which indicates a dominantly strike slip movement along this transverse fault (Fig. 23). The displaced basaltic ridge near Tejpur is locally known as the ‘Khaseli Dungan’, which literally

means a 'shifted hill' (Fig. 23). This fault shows a right lateral offset of the NSF for about 1 km. The presence of the fault is evidenced by the straight channel of the Madhumati River and the formation of a large, deeply-incised and compressed meander in alluvium as it emerges from the uplands. The slickensides exposed along the fault plane in basaltic rocks, on the left bank of the river, suggest oblique slip movement (Fig. 23). The incision of the river is of the order of 40 m.

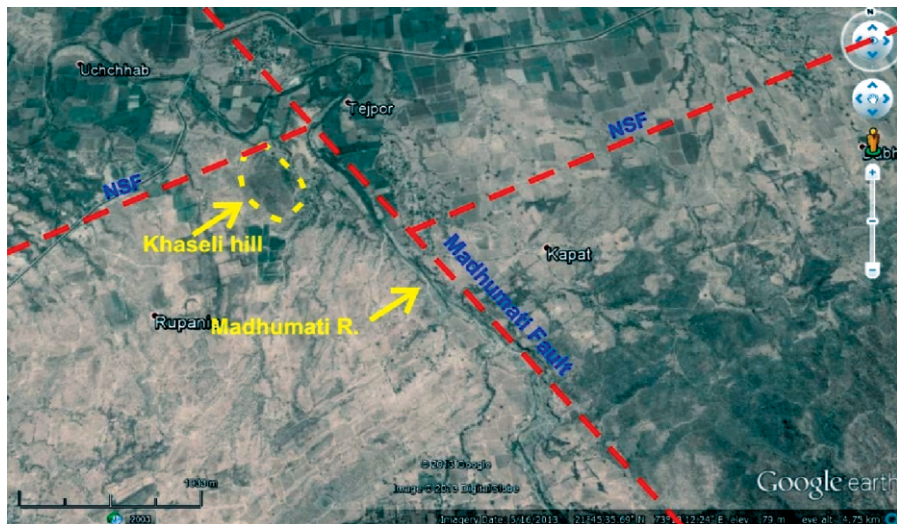


Fig. 23.

Fig. 23. Google Earth image of NSF zone and its structural elements near Madhumati River. Note the straight course of Madhumati River along the NNW-SSE trending transverse fault and the compressed meander near Tejpur.

The large entrenched meander near Tejpur has exposed a 35 m cliff (Fig. 23). Downstream of Tejpur, the river flows towards NW with several entrenched meanders in the alluvial zone (Fig. 23). At Rajpardi, the river takes a north-westerly turn because of the influence of the Rajpardi fault.

In the alluvial zone of Madhumati river, the late Quaternary fluvial deposits are characterized by a regular and cyclic sequence of sand and gravel. The clasts of the gravel bed consist of basalt derived from the upland. The clasts are poorly sorted and the matrix is mainly coarse to medium sand. In the lower reaches these cyclic sequences of sand and gravel overlie the clay horizon. The best and highest exposed section in the alluvial zone of the Madhumati River basin is located at Tejpur. Here the Quaternary sediments abruptly abut against the Trappean rocks along the NSF.

The average thickness of the section on the right bank is about 35 m. The oldest exposed sediment is gravel, its thickness being about 1 m. This bed is succeeded by 5 m thick pedogenised sand which in turn is overlain by 2 m thick gravel, showing no stratification. This bed is succeeded by 5 m massive sand, which in turn is overlain by 7 m horizontally-stratified gravel, embedded with cobbles. Within this layer sand lenses of about 1 m thickness are present. This bed is overlain by 3 m thick, weakly pedogenised sandy silt, which in turn is overlain by 3 m weakly stratified gravel. This bed is overlain by a 3 m thick massive sand over which a 4 m gravel bed rests. The whole sequence is capped by 1 m topsoil.

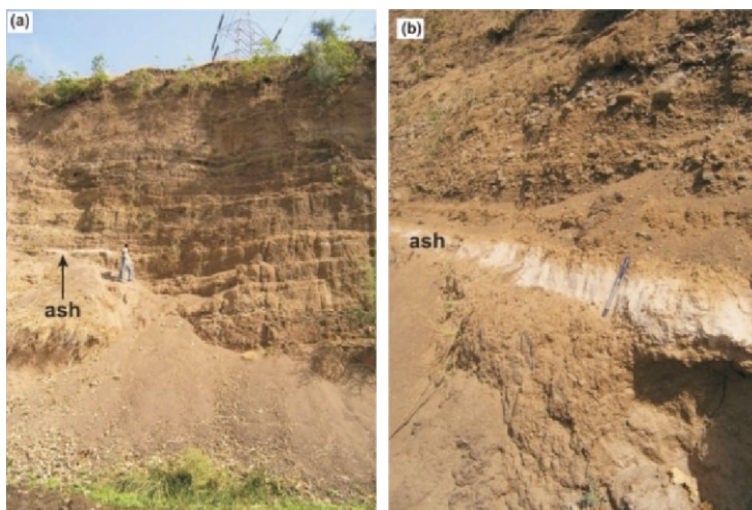


Fig. 24.

*The cliff along the Madhumati River at Tejpur. Note the position of volcanic ash unit. (A) distant view, (B) close view (after Raj et al., 2008).*

A most interesting feature in the Tajpur section is the occurrence of a volcanic ash layer within the Quaternary alluvial succession (Fig. 24). This ash bed is correlated with the Youngest Toba tuff (Raj, 2008). The ash is unconsolidated, well-sorted, homogenous and friable to the extent of getting to fine powdery material. Glass shards make up 90% of the ash although pumice fragments are also present. Accessory minerals include quartz, feldspars, biotite and occasional zircon. The details of the micro-structures of glass shard and pumice shard have been brought out very clearly by the SEM studies. The shape of glass shards ranges from blocky, cusped, flat or platy, triangular, tri-radiate or multi-junctional (Fig. 25). Most of them show a typical bubble wall structure, which is indicative of a magmatic type of eruption.

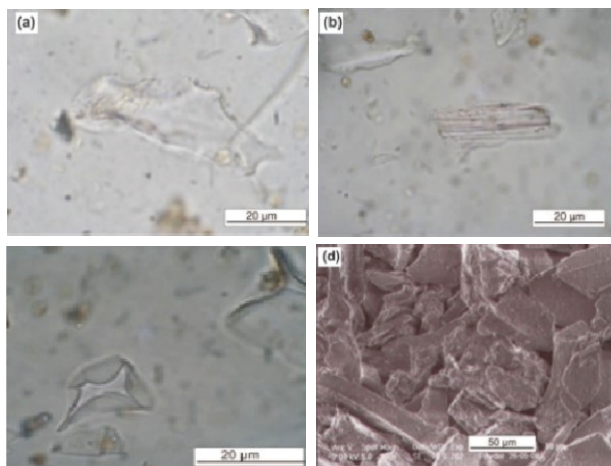


Fig. 25.

*SEM photographs (after Raj et al., 2008) of the volcanic ash deposit. (A) Glass shard showing typical conchoidal fracture. (B) Light, porous pumice shard consisting of parallel vesicles seen as long stretched thin capillary tube. (C) Shard showing tri-radiate junction wall of three bubbles. (D) Glass shard of different size and shape showing smooth and conchoidal surface.*

The Toba volcanic event is one of the largest eruptions during the Quaternary period (Schultz et al., 2002). This volcanic mega-eruption (Rose and Chesner, 1987, 1990; Knight et al., 1986; Acharyya and Basu, 1993) took place some 70,000 years ago in the northern Sumatra within the Indonesian archipelago, when a major shift was taking place in global climate from the interglacial marine isotopic stage (MIS) 5 to glacial MIS 4 (Ninkovich et al., 1978). This Toba volcanic event was more than two orders of magnitude larger than any historical eruption, and produced at least 3000 km<sup>2</sup> of dense rock-equivalent rhyolite magma ( $7 \times 10^{15}$ ) and more than 800 km<sup>3</sup> of ash (Viseras and Fernandez, 1995). It is estimated that at least 1% of the Earth was covered by more than 10 cm of ash known as Youngest Toba Tuff (YTT). A widespread occurrence of tephra bed is reported, e.g., from the eastern and the western parts of the Indian subcontinent (Acharyya and Basu, 1993; Ninkovich et al., 1978; Chesner et al., 1991), the Arabian Sea (Schultz et al., 1998), the Indian Ocean (Pattan et al., 1999) and the South China Sea (Buhring et al., 2000; Song et al., 2000). The Toba event is believed to have affected the global climate system (Singurdsson, 1990). It might have also been responsible for the shift to glacial climate (Chesner et al., 1991; Rampino and Self, 1992, 1993).

#### Stop 4: Karjan Dam Section

Karjan River is a major tributary of the Narmada River, and has the largest tributary drainage basin within the lower Narmada basin. The effect of the ENE-WSW trending NSF is evident in the upland zone of the river where the basaltic flows are tilted southward. The stream course is not only controlled by the NSF, but also by the NNW-SSE trending Karjan Fault, especially in the alluvial zone (Fig. 13). Activities along the Karjan Fault make the basin asymmetrical, tilting it towards the west.

In the upland area of the Karjan River southward-dipping basaltic flows could be seen. The dipping flows represent part of the tilted block that is attributed to the tectonic movements along the NSF. Exposed section reveals a terrace surface at a height of 58 m from the present-day channel (Fig. 26). The sediments are dominantly sand and silty sand deposits. Calcite sheets and nodules occur in the middle of the section. OSL dating of the upper silty sand layer has yielded a date of  $32.7 \pm 3.9$  Ka (Fig. 26).

On the basis of sediment fabric, grain size and lithofacies association, the exposed sediments at Karjan Dam site can be correlated with the sediments in the downstream. However, there is a significant difference between the altitudes at which sediments are exposed, which could be attributed to displacement along the NSF during the Early Holocene time (Chamyal et al., 2002).

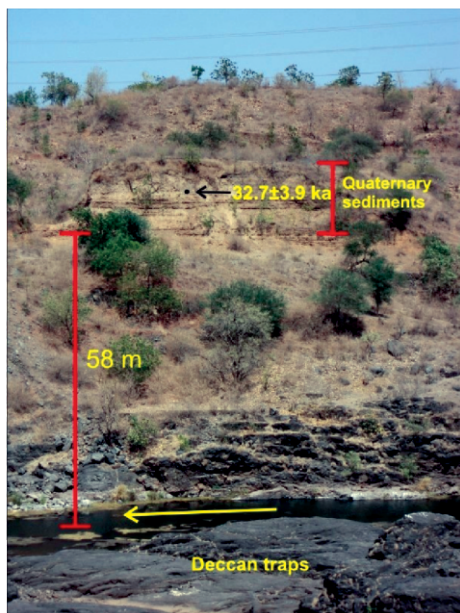


Fig. 26.  
Cliff on the right bank of Karjan River near Karjan Dam. Arrow indicates downstream direction of the river. Note the elevation of late Quaternary sediments above the incised bedrock comprising basaltic flows of Deccan Trap Formation.

**Day 5: 16/11/2017**

**Vadodara to Tavra, Bharuch, Raniour, Karad and back to Vadodara**

**Departure by Flight to New Delhi**

**Stay at New Delhi.**

The estuarine zone of the Narmada River may not be as large as that of the Ganga or the Brahmaputra, but is interesting, nevertheless. A visit to some of the sites along the narrow estuary will help to appreciate the geomorphic processes interacting in the area over the millennia. We first provide a short overview of the characteristics of sedimentary sequences along the estuary and their depositional environment.

### **Estuarine Sequences of the Narmada River**

The sediments comprising the valley fill terrace surface ( $S_4$ ) are exposed in 5-10 m high incised cliffs in the lower Narmada basin. These comprise two lithofacies, the tidal estuarine facies in the lower reaches and the fluvial sand facies in the upper reaches. The tidal estuarine facies is dominated by tidal carbonaceous mud with intervening fine to medium estuarine sand, showing parallel lamination. Micro-palaeontological investigations on the muddy horizons have yielded a rich assemblage of shallow marine foraminifers (Chamyal et al., 2002). The sands show ripple and cross-stratification with abundant mud laminae, flasers and drapes. The sands also show parallel bedding and bi-directional cross-stratification. Overall, the estuarine terrace sequence is dominated by tidal mud, which suggests their deposition in a tide-dominated estuarine condition. Similar facies is found in the present estuary also, which is also tide-dominated (Nigam, 1984). The tripartite (coarse-fine-coarse) facies assemblage, which is characteristic of wave-dominated estuaries (Darymple et al., 1992), is not found in the sediments. In tide-dominated estuaries, the muddy sediments accumulate primarily in the tidal flats and sand marshes, while sand is deposited in the tidal channels that run along the length of the estuary (Woodroffe et al., 1989; Darymple et al., 1992). The geomorphic setting suggests that these sediments were deposited as an aggrading transgressive tidal estuarine facies, transforming the fluvial incised valley into an estuary (Chamyal et al., 2002).

Upstream of the tidal estuarine terraces, comparable fluvial terraces occur right up to the upland zone with identical geomorphic setting. These terraces mainly consist of horizontally-stratified fluvial silty sand ( $Sh$ ). The lateral accretion surfaces are completely absent, indicating aggradation of the incised valley through vertical accretion when the lower reaches of the river were undergoing tidal estuarine sedimentation. However, the change from a fluvial to a tidal facies is not sharply defined and appears to be transitional (Chamyal et al., 2002).

### Stop 1: Tavra- Bharuch Section

At Tavra, an 8 m Holocene section, comprising estuarine sediments, is exposed along the Narmada River. It extends downstream up to Bharuch. The 0.5 m thick clay at the base is dark in colour and is rich in organic materials. This is overlain by 4 cm of sandy layer in the form of a lens, over which a silty clay bed (1.2 m) is exposed. An organic-rich clay deposit occurs above it for 3.5 m thickness, and is overlain by a 15 cm lens of sandy silt. This is followed upwards by a dark, organic-rich laminated clay for 20 cm. The laminated clay is overlain by 30cm of brownish silty clay, over which another laminated clay band of 20cm thickness occurs. Over this clay bed occurs a 67 cm thick silty clay bed. Above the silty clay 11cm of clay is exposed. This is overlain by 4 cm layer of silt and over it a 15 cm of clay. A 1.2 cm of dark organic rich laminated clay, dark brown to blackish in colour overlies the thin clay layers. This is overlain by silty sand (1.25 m). The top 45 cm is marked by sand.

### Stop 2: Ranipura Section

The terrace deposits along the lower Narmada valley are generally 3-4 m thick. They are mainly composed of weakly-laminated sand and silt with intermittent thin clay layers and organic inter-stratifications. The valley carries water periodically, especially during the SW monsoon. Incision has led to the formation of the terrace, which currently is inundated during high-magnitude flood events. Therefore, erosion and reworking of terrace sediments and organic material cannot be ruled out. On the basis of stratigraphic and sedimentological characteristics, Alpa Sridhar et al. (2015) divided these terrace deposits into four units: U-I (lowermost), U-II, U-III and U-IV (uppermost). The lowermost unit U-I (430-460 cm) is dominantly composed of grey medium to coarse sand (96%), with thin horizons of finer sediments (60% silt, 40% clay), and the base is not exposed (*Fig. 27*). No sedimentary structure is seen, and very little organic matter is present. U-II is a 115 cm thick, laterally continuous layer consisting of finely-laminated silt and clay. The contact between U-I and U-II is sharp. The bottom 65 cm of U-II comprises predominantly of black organic-rich clayey horizons with intermittent millimetre-scale silt bands. This is overlain by 50 cm thick inter-layered sand and silt horizon with fine, brownish organic-rich sediment, abundant rootlets, leaf and woody debris, including tree stumps. These layers show mottling and blocky character due to oxidation and fluctuating water levels. The silt fraction is ~55%. This organic-rich unit is overlain by U-III, the thickest unit (~240 cm), with an abrupt contact with U-II. The sediments are brown to yellow and partially pedogenized, showing a typical blocky character. The layers are faintly laminated and occur as fine sand and silt couplets. In the lower half of the unit, the sediments are composed of 3-8% sand, 50-60% silt and 37-42% clay, indicating an overall dominance of silt. In the upper half, clay content increases significantly (up to 50%) at the expense of silt. U-IV (~70 cm), the uppermost part, has centimetre-scale sand and

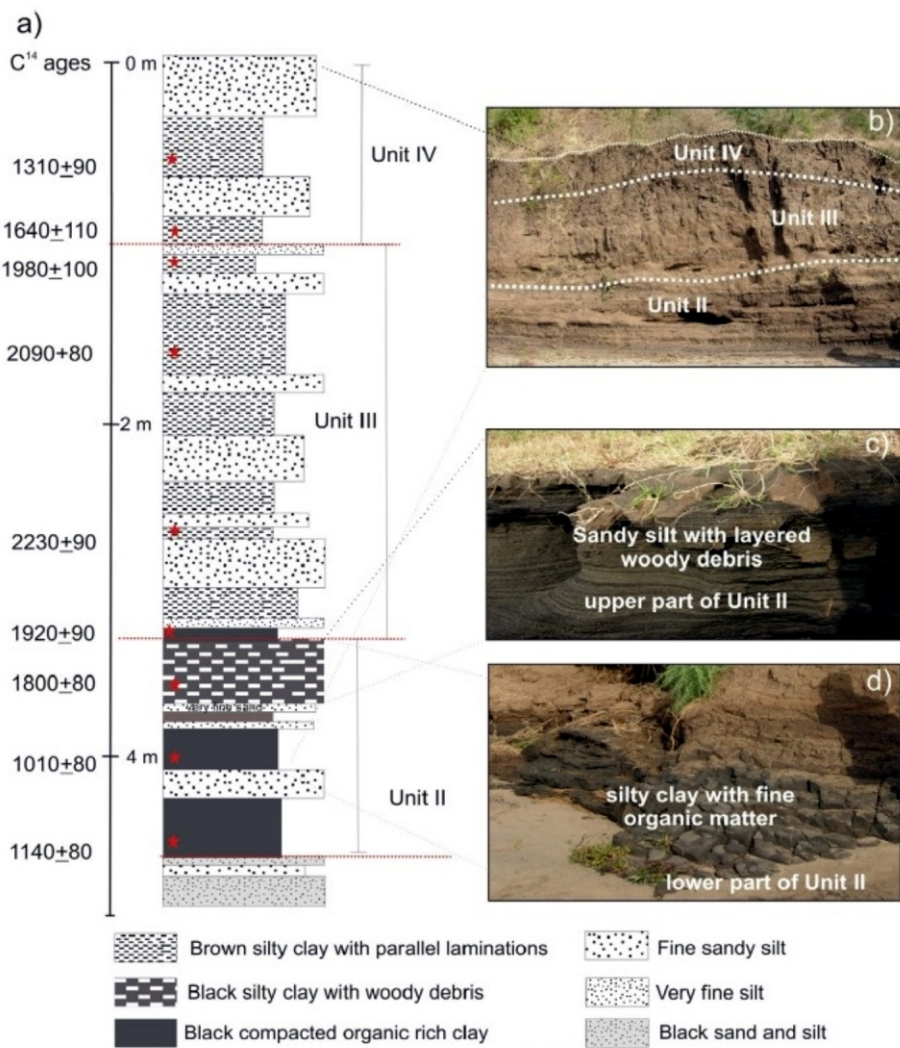


Fig. 27.

(A) Generalized litholog of the late Holocene terrace sediments exposed at Ranipura showing four distinct units. Also shown are the close views of (B) the section showing unit II, III and IV, (C) woody debris-rich upper part of unit II, and (D) organic matter-rich black clay in the lower part of unit II (after Alpa Sridhar et al., 2015).

silt laminations, without any organic-rich horizon. The unit is weakly pedogenized and highly bioturbated.

On the basis of proxy data and chronology, four climatic phases (I-IV) during the last two millennia have been interpreted (Alpa Sridhar et al, 2015). The first phase (prior to 2185 cal BP) has been inferred as a wet phase under a strong monsoon regime (Fig. 28). The coarser sediments and the negligible palynomorph yield during this phase indicate deposition under a high-energy fluvial condition, possibly a stream channel environment. During phase II, ~2200-1800 cal BP, low precipitation and related reduction in sediment influx resulted in enhanced tidal conditions and a wider than present estuary. During phase III, the sediment influx increased, along with enhanced monsoon precipitation. During phase IV, the sediments were deposited in stagnant water in a freshwater back-swamp with intermittent oxidizing and reducing conditions and fluctuating water table conditions.

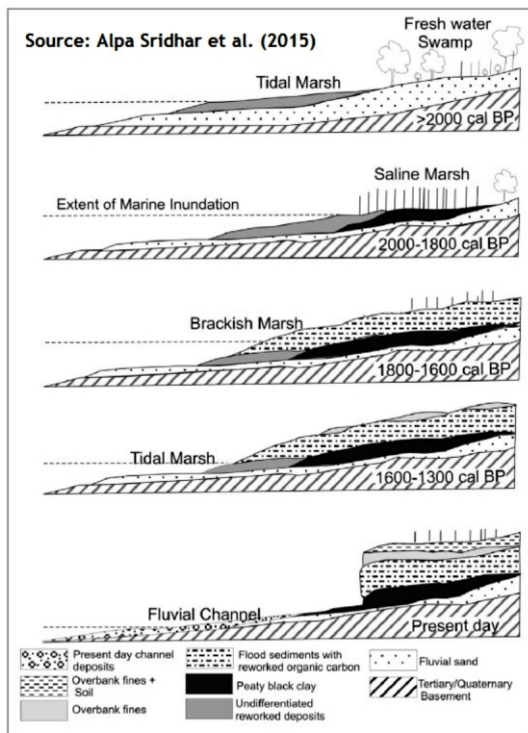


Fig. 28.

*Depositional model of the Narmada estuarine zone during late Holocene (after Alpa Sridhar et al., 2015).*

*Note the inundation of the Narmada lowland by sea water leading to tidal marsh conditions till 1809 ca.*

All through, the sediments were deposited as fine sand and silt couplets, often with algal cysts and well-preserved organic matter derived from the cuticles of higher land plants. These are indicative of proximal depositional environment, rapid burial, and good accommodation potential, as supported by the chronological results. The present-day environment is facilitating multiple flooding events within a short time span. Construction of a depositional model of the Narmada lowland during the late Holocene period reveals a gradual strengthening of southwest monsoon after ~3500

cal BP, with a short pulse of dry climatic condition (~3238 - ~2709 cal BP). This was followed by climate somewhat similar to the present. Marine inundation of the lowland by sea water took place between ~2000 and 1800 cal BP, leading to tidal marsh conditions. This was followed by withdrawal of the tidal condition and large terrestrial sediment influx between 1692 and 1487 cal BP, which is coeval with a wet phase.

### **Stop 3: Palaeo-bank of Narmada River near Karad**

In the westernmost part, the NSF is represented by steep escarpments along the Tertiary highlands, whereas further west it is expressed as a palaeo-bank of the Narmada River. The entire Tertiary sequence is folded and faulted. In this segment, the exposed Tertiaries exhibit linear anticlinal structure, trending SW to WSW, plunging SW to WSW and flanked by reverse faults along the southern limbs. The Tertiary sequence ranges in age from Paleocene to Mio-Pliocene, and is dominated by rudaceous to calcareous facies and highly ferruginous, cyclic sedimentation of calcareous sandstone and marls, calcareous clays, forminiferal limestone and fossiliferous beds.

The palaeo-bank at Karad is marked by straight linear alluvial cliffs formed in the Quaternary sediments. It is formed by the migration of Narmada River to the NW to its present course, and represents an abandoned left bank of the river when it was flowing further to the SE. Since then the river has migrated by about 6 km to the NW, especially due to tilting caused by the upliftment of the Jhagadia-Ankleshwar area. The linearity of the feature suggests the presence of a fault along this palaeo-bank. Previous seismic studies suggested the presence of reverse fault along the palaeo-bank with the down-throw side to the NW and the upthrow side to the SE side (Agarwal et al., 1986).

## References

- Acharyya, S. K. and Basu, P. K. 1993. Toba ash on the Indian subcontinent and its implications for the correlation of late Pleistocene alluvium. *Quaternary Research*, 40: 10-19.
- Acharyya, S. K., Kayal, J. R., Roy, A. and Chaturvedi, R. K. 1998. Jabalpur earthquake of May 22, 1997: constraint from an aftershock study. *Journal of the Geological Society of India*, 51: 295- 304.
- Acharyya, S.K. and Roy, A. 2000. Tectonothermal history of the central Indian tectonic zone and reactivation of major faults/shear zones. *Journal of the Geological Society of India*, 55: 239–256.
- Agarwal, G. C. 1986. Structure and tectonics of exposed Tertiary rocks between Narmada and Kim rivers in South Gujarat. *Journal of the Geological Society of India*, 27: 531–542.
- Agarwal, B.N.P., Das, L.K., Chakraborty, K. and Sivaji, C.H. 1995. Analysis of the Bouguer anomaly over central India: a regional perspective. *Memoir, Geological Society of India*, 31: 469–493.
- Ahmad, F. 1986. Geological evidence bearing on the origin of the Rajasthan desert. *Proceedings, Indian National Science Academy*, 52A (6): 1285-1306.
- Allchin, B., Goudie, A., and Hegde, K.T.M. 1978. *The Prehistory and Palaeogeography of the Great Indian Desert*. Academic Press, London, 370p.
- Allen, C. R. 1975. Geological criteria for evaluating seismicity. *Geological Society of America Bulletin*, 86: 1041-1057.
- Autin, W. J. 1996. Pleistocene stratigraphy in the southern Lower Mississippi Valley. *Engng. Geol. v. 45*, pp. 87–112.
- Badam, G.L., Ganjoo, R.K. and Salahuddin. 1986. Preliminary taphonomical studies of some Pleistocene fauna from the Central Narmada Valley, Madhya Pradesh, India. *Palaeogeography, Palaeoclimatology, Palaeoecology*, 53: 335-348.

Bhandari, S., Raj, R., Maurya, D. M. and Chamyal, L. S. 2001. Formation and erosion of Holocene alluvial fans along the Narmada-Son Fault around Rajpipla in the lower Narmada basin, western India. *Journal of the Geological Society of India*, 55: 595-610.

Bhandari, S., Maurya, D.M. and Chamyal, L.S. 2005. Late Pleistocene alluvial plain sedimentation in Lower Narmada Valley, western India: palaeoenvironmental implications. *Journal of Asian Earth Sciences*, 24: 433–444.

Bhattacharji, S., Chatterjee, N. and Wampler, J. M. 1996. Zones of Narmada-Tapi rift reactivation and Deccan volcanism: geochronological and geochemical evidence. In: Deshmukh, S.S., Nair, K.K.K. (Eds.), *Deccan Basalts*. Gondwana Geological Society, Nagpur, pp. 329–340.

Biswas, S. K. .1987. Regional tectonic framework, structure and evolution of western marginal basins of India. *Tectonophysics*, 135: 307-327.

Blair, T.C. and Bilodeau, W.L. 1988. Development of tectonic cyclothems, in rift, pull-apart and foreland basins: sedimentary response to episodic tectonism. *Geology*, 16: 517-520.

Blair, T.C. and McPherson, J. 1994. Alluvial fans and their natural distinction from rivers based on morphology, hydraulic processes, sedimentary processes and facies. *Journal of Sedimentary Petrology*, 64: 450-489.

Blum, M.D., Guccione, M.J., Wysocki, D.A., Robnett, P.C. and Rutledge, E.M. 2000. Late Pleistocene evolution of the lower Mississippi valley, southern Missouri to Arkansas. *Geological Society of America Bulletin*, 112: 221–235.

Brown, G.H. and Plint, A.G. 1994. Alternating braidplain and lacustrine deposition in a strike-slip setting: the Pennsylvanian Boss Point Formation of the Cumberland basin, Maritime Canada. *Journal of Sedimentary Petrology*, 64: 40-59.

Buhring, C., Sarnthein, M. and LEG 184 Shipboard Party. 2000. Toba ash layers in the South China Sea: Evidence for contrasting wind directions during eruption ca. 74 ka. *Geology*, 28: 275–278.

Bull, W.B. 1991. *Geomorphic Responses to Climate Change*. Oxford Univ. Press, New York, 327p.

Chandra, U. 1977. Earthquakes of Peninsular India: A seismotectonic study. *Bulletin of the Seismic Society of America*, 65: 1387-1413.

Chamyal, L.S., Khadkikar, A.S., Malik, J.N. and Maurya, D.M. 1997. Sedimentology of the Narmada alluvial fan, western India. *Sedimentary Geology*, 109: 263-279.

Chamyal, L. S. and Maurya, D. M. 2002. Status of Quaternary geological studies in parts of India: A synthesis. *Indian Minerals*, 56: 1-26.

Chamyal, L. S., Maurya, D. M., Bhandari, S. and Raj, R. 2002. Late Quaternary geomorphic evolution of Lower Narmada Valley, western India: Implications for neotectonic movements along the Narmada-Son Fault. *Geomorphology*, 46: 177-202.

Chamyal, L. S., Maurya, D.M. and Raj, R. 2003. Fluvial systems of the drylands of western India: a synthesis of late Quaternary environmental and tectonic changes. *Quaternary International*, 104: 69-86.

Chappell, J. and Shackleton, N.J. 1986. Oxygen isotopes and sea level. *Nature*, 324: 137-140.

Chesner, C. A., Rose, W. I., Deino, A., Drake, R. and Westgate, J. A. 1991. Eruptive history of Earth's largest Quaternary caldera (Toba, Indonesia) clarified. *Geology*, 19: 200-203.

Choubey, V.D. 1971. Narmada-Son lineament, India. *Nature*, 2332: 38-40.

Coleman, J.M. 1969. Brahmaputra River: Channel processes and sedimentation. *Sedimentary Geology*, 3: 129-239.

Darymple, R.W., Zaitlin, B.A. and Boyd, R. 1992. Estuarine facies models: Conceptual basis and stratigraphic implications. *Journal of Sedimentary Petrology*, 62: 1130-1146.

Dury, G. H. 1970. General theory of meandering valleys and underfit streams. In: G. H. Dury (Ed.), *Rivers and River Terraces*. Macmillan, London, pp. 264-275.

Ely, L.L., Enzel, Y., Baker, V.R., Kale, V.S. and Mishra, S. 1996. Changes in the magnitude and frequency of late Holocene monsoon floods on the Narmada river, central India. *Geological Society of America Bulletin*, 108: 1134-1148.

Fuller, I.C., Macklin, M.G., Lewin, J., Passmore, D.G. and Wintle, A.G. 1998. River response to high frequency climate oscillations in southern Europe over the past 200 k.y. *Geology*, 26: 275-278.

Graf, W.L. 1988. *Fluvial Processes in Dryland Rivers*. Springer, Berlin.

Goudie, A.S. 1983. Calcrete. In: A. S. Goudie and K. Pye (Eds), *Chemical Sediments and Geomorphology*. Academic Press, London, pp. 93-131.

Gupta, A., Kale, V.S. and Rajaguru, S.N. 1999. The Narmada River, India, through space and time. In: A. J. Miller and A. Gupta (Eds.), *Varieties of Fluvial Form*. John Wiley and Sons, pp. 113-143.

Gupta, H.K., Chadha, R.K., Rao, M.N., Narayana, B.L., Mandal, P., Ravikumar, M. and Kumar, N. 1997. The Jabalpur earthquake of May 22, 1997. *Journal of the Geological Society of India*, 50: 85-91.

Gupta, H.K., Mohan, I. and Hari Narain. 1972. The Broach earthquake of March 23, 1970. *Bulletin of the Seismic Society America*, 62: 47-61.

Hagen, E.S., Schuster, M.W. and Furlong, K.P. 1985. Tectonic loading and subsidence of intermontane basins: Wyoming foreland province. *Geology*, 13: 585-588.

Hashimi, N. H., Nigam, R., Nair, R. R. and Rajagopalan, G. 1995. Holocene sea level fluctuations on western Indian continental margin: An update. *Journal of the Geological Society of India*, 46: 157-162.

Jackson, R. G. 1978. Preliminary evaluation of lithofacies models for meandering alluvial streams. In: A. D. Miall (Ed.), *Fluvial Sedimentology*. Memoir, Canadian Society of Petroleum Geologists, 5: 543-576.

Jain, M., Woodcock, N.H. and Tandon, S.K. 1998. Neotectonics of western India: evidence from deformed fluvial sequences, Mahi river, Gujarat. *Journal of the Geological Society of London*, 155: 897-901.

Jordan, T. E. 1981. Thrust loads and foreland basin evolution, Cretaceous, western United States. *Bulletin of the American Association of Petroleum Geologists*, 15: 2500-2520.

Joshi, P., Maurya, D. M. and Chamyal, L. S. 2013a. Morphotectonic segmentation and spatial variability of neotectonic activity along the Narmada-son Fault (NSF), Gujarat, western India: Remote sensing and GIS analysis. *Geomorphology*, 180: 292-306.

Joshi, P., Maurya, D. M. and Chamyal, L. S. 2013b. Tectonic and climatic controls on late Quaternary Bajada sedimentation along Narmada-Son Fault (NSF), Gujarat, Western India. *International Journal of Sediment Research*, 28: 66-76.

Juyal, N., Raj, R., Maurya, D.M., Chamyal, L.S. and Singhvi, A.K. 2000. Chronology of Late Pleistocene environmental changes in the lower Mahi basin, western India. *Journal of Quaternary Science*, 15: 501-508.

Juyal, N., Kar, A., Rajaguru, S.N and Singhvi, A.K. 2003. Luminescence chronology of aeolian deposition during the Late Quaternary on the southern margin of Thar Desert, India. *Quaternary International*, 104: 87-98.

Juyal, N., Chamyal, L. S., Bhandari, S., Maurya, D. M. and Singhvi, A. K. 2004. Environmental changes during Late Pleistocene in Orsang basin, western India. *Journal of the Geological Society of India*, 64: 471-179.

Juyal, N., Chamyal, L.S., Bhandari, S., Bhushan, R. and Singhvi, A.K. 2006. Continental record of the southwest monsoon during the last 130 ka: evidence from the southern margin of the Thar Desert, India. *Quaternary Science Reviews*, 25: 2632-2650.

Kaila, K.L., Krishna, V.G. and Mall, D. 1981. Crustal structure along Mehmadaabad–Billimora profile in the Cambay basin, India from deep seismic soundings. *Tectonophysics*, 76: 99-130.

Kale, V.S. and Rajaguru, S.N. 1987. Late Quaternary alluvial history of the Northwestern Deccan Upland region. *Nature*, 325: 612-614.

Kale, V. S., Ely, L. L., Enzel, Y. and Baker, V. R. 1994. Geomorphic and hydrologic aspects of monsoon floods on the Narmada and Tapi rivers in Central India. *Geomorphology*, 10: 157-168.

Kale, V.S. 1999. Long-period fluctuations in monsoon floods in the Deccan Peninsula. *Journal of the Geological Society of India*, 53: 5–15.

Kale, V.S., Mishra, S. and Baker, V.R. 2003. Sedimentary records of palaeofloods in the bedrock gorges of the Tapi and Narmada rivers, central India. *Current Science*, 84: 1072-1079.

Kershaw, A. P. and Nanson, G.C. 1993. The last full glacial cycle in the Australian region. *Global and Planetary Change*, 7: 1-9.

Khadkikar, A.S., Merh, S.S., Malik, J.N. and Chamyal, L.S. 1998. Calcretes in semi-arid alluvial systems: Formative pathways and sinks. *Sedimentary Geology*, 116: 251-260.

Knight, M. D., Walker, G. P. L., Ellwood, B. B. and Diehl, J. F. 1986. Stratigraphy, paleomagnetism, and magnetic fabric of the Toba Tuffs: Constraints on the sources and eruptive styles. *Journal of Geophysical Research B*, 91: 10,355-10,382.

Kotlia, B.S., Sharma, C., Bhalla, M.S., Rajagopalan, G., Subrahmanyam, K., Bhattacharya, A. and Valdiya, K.S. 2000. Palaeoclimatic conditions in the late Pleistocene Wadda Lake, eastern Kumaun Himalaya (India). *Palaeogeography, Palaeoclimatology, Palaeoecology*, 162: 105-118.

Kraus, M.J. and Middleton, L.T. 1987. Contrasting architecture of two alluvial suites in different structural settings. In: F.G. Ethridge, R.M. Flores and M.D. Harvey (Eds.), *Recent Developments in Fluvial Sedimentology*. Special Publication, Society for Economic Paleontology and Mineralogy, 39: 253–262.

Kraus, M.J. 1992. Alluvial response to differential subsidence: Sedimentological analysis aided by remote sensing. Willwood Formation (Eocene), Bighorn Basin, Wyoming, USA. *Sedimentology*, 39: 455-470.

Kraus, M.J. and Aslan, A. 1993. Eocene hydromorphic palaeosols: significance for interpreting ancient floodplain processes. *Journal of Sedimentary Petrology*, 63: 453-463.

Kraus, M.J. 1997. Early Eocene alluvial paleosols: Pedogenic development, stratigraphic relationships and paleosol/landscape associations. *Palaeogeography, Palaeoclimatology, Palaeoecology*, 129: 387-406.

Kusumgar, S., Raj, R., Chamyal, L.S. and Yadav, M.G. 1998. Holocene palaeoenvironmental changes in the Mahi river basin, Gujarat, Western India. *Proceedings, Radiocarbon Journal (16th International 14C Conference; W.G. Mook and J. Plitch, Eds.)*, 40: 819-823.

Macklin, M.G., Fuller, I.C., Lewin, J., Maas, G.S., Passmore, D.G., Rose, J., Woodward, J.C., Black, S., Hamlin, R.H.B. and Rowan, J.S. 2002. Correlation of fluvial sequences in the Mediterranean basin over the last 200 ka and their relationship to climate change. *Quaternary Science Review*, 21: 1633-1641.

Maddy, D., Bridgeland, D.R. and Westway, R. 2001. Uplift-driven valley incision and climate controlled river terrace development in the Thames valley, U.K. *Quaternary International*, 79:23-36.

Malik, J.N., Khadkikar, A.S. and Merh, S.S. 1999. Allogenic control on Late Quaternary continental sedimentation in the Mahi river basin, western India. *Journal of the Geological Society of India*, 53: 299-314.

Marriott, S. B. and Wright, V. P. 1993. Palaeosols as indicators of geomorphic stability in two Old Red Sandstone alluvial suites, south Wales. *Journal of the Geological Society, London*, 150: 1109-1120.

Maurya, D.M., Chamyal, L.S. and Merh, S.S. 1995. Tectonic evolution of central Gujarat alluvial plains, Western India. *Current Science*, 69: 610-613.

Maurya, D.M., Malik, J.N., Raj, R. and Chamyal, L.S. 1997a. Soft sediments deformation in the Quaternary sediments of the Lower Mahi river basin, Western India. *Current Science*, 72: 519-522.

Maurya, D.M., Malik, J.N., Raj, R. and Chamyal, L.S. 1997b. The Holocene valley fill terraces in the Lower Mahi valley, Western India. *Current Science*, 73: 539-542.

Maurya, D.M., Raj, R., and Chamyal, L.S. 1998. Seismically induced deformational structures from Mid-Late Holocene terraces in the lower Mahi valley, Gujarat. *Journal of the Geological Society of India*, 51: 755-758.

Maurya, D.M., Raj, R. and Chamyal, L.S. 2000. History of tectonic evolution of Gujarat alluvial plains, western India during Quaternary: A review. *Journal of the Geological Society of India*, 55: 343-366.

Maurya, D. M., Bhandari, S., Thakkar, M. G. and Chamyal, L.S. 2003. Late Quaternary fluvial sequences of southern Mainland Kachchh, western India. *Current Science*, 84: 1056-1064.

McCarthy, T.S. and Metcalfe, J. 1990. Chemical sedimentation in the semi-arid environment of the Okavango Delta, Botswana. *Chemical Geology*, 89: 157-178.

Merh, S.S. 1993. Neogene Quaternary sequence in Gujarat: A review. *Journal of the Geological Society of India*, 21: 259-276.

Miall, A.D. 1978. Lithofacies types and vertical profile models in braided river deposits: A summary. In: A.D. Miall (Ed.), *Fluvial Sedimentology*. Memoir, Canadian Society of Petroleum Geologists, 5: 597-604.

Miall, A.D. 1985. Architectural element analysis: A new method of facies analysis applied to fluvial deposits. *Earth Science Reviews*, 22: 261-308.

Miall, A.D. 1996. *The Geology of Fluvial Deposits*. Springer-Verlag, Berlin Heidelberg, 581p.

Murthy, J.V.S. 1975. In, *Proceedings of National Symposium on Hydrology*. University of Roorkee, Roorkee, India. pp. 2-5.

Nanson, G.C. and Croke, J.C. 1992. A genetic classification of floodplains. *Geomorphology*, 4: 459-486.

Ninkovich, D., Shackleton, N. J., Abdel-Monem, A. A., Obradovich, J. D. and Izett, G. 1978. K-Ar age of the Pleistocene eruption of Toba, north Sumatra. *Nature*, 276: 574-577.

Pant, R.K. and Chamyal, L. S. 1990. Quaternary sedimentation pattern and terrain evolution in the Mahi river, Gujarat, India. *Proceedings of the Indian National Science Academy*, 56: 501-511.

Pant, R.K. and Juyal, N. 1993. Late Quaternary coastal instability and sea level changes: new evidence from Saurashtra coast, Western India. *Zeitschrift fur Geomorphologie*, 3: 29-40.

Pye, K. 1983. Red beds. In, A.S. Goudie and K. Pye (Eds.), *Chemicals Sediments and Geomorphology*. Academic Press, London, pp. 227-263.

Quittmeyer, R. C. and Jacob, K. H. 1979. Historical and modern seismicity of Pakistan, Afghanistan, northwestern India and southeastern India. *Bulletin of the Seismological Society of India*, 69: 773-823.

Raj, R. 2008. Occurrence of volcanic ash in the Quaternary alluvial deposits, lower Narmada basin, Western India. *Journal of Earth System Science*, 117: 41-48.

Raj, R. and Chamyal, L.S. 1998. Microfauna from a Holocene valley fill terrace, Lower Mahi basin, Gujarat. *Journal of the Palaeontological Society of India*, 43: 55-67.

Raj, R., Maurya, D. M. and Chamyal, L. S. 1998. Late Quaternary sea-level changes in Western India: Evidence from Lower Mahi Valley. *Current Science*, 74: 910-914.

- Raj, R., Maurya, D.M. and Chamyal, L.S. 1999. Tectonic control on distribution and evolution of ravines in the Lower Mahi valley, Gujarat. *Journal of the Geological Society of India*, 53: 669-674.
- Radhakrishna, B.P. and Ramakrishnan, M. 1988. Archaean-Proterozoic boundary in India. *Journal of the Geological Society of India*, 32: 263-278.
- Rajaguru, S.N., Gupta, A., Kale, V.S., Ganjoo, R.K., Ely, L.L., Enzel, Y. and Baker, V.R. 1995. Channel form and processes of the flood-dominated Narmada River, India. *Earth Surface Processes and Landforms*, 20: 407-421.
- Rampino, M. R. and Self, S. 1992. Volcanic winter and accelerated glaciations following the Toba super-eruption. *Nature*, 359: 50-52.
- Rampino, M. R. and Self, S. 1993. Climate-volcanism feedback and the Toba Eruption of >74,000 years ago. *Quaternary Research*, 40: 269-280.
- Retallack, G.J. 1990. *Soils of the Past: An Introduction to Palaeopedology*. Unwin Hyman, London, 520p.
- Rose, W. I. and Chesner, C. A. 1987. Dispersal of ash in the great Toba eruption, 75 ka. *Geology*, 15: 913-917.
- Rose, W. I. and Chesner, C. A. 1990. Worldwide dispersal of ash and gases from Earth's largest known eruption: Toba, Sumatra, 75ka. *Palaeogeography, Palaeoclimatology, Palaeoecology*, 89: 269-275.
- Roy, T.K. 1990. Structural styles in southern Cambay basin and role of Narmada geofracture in the formation of giant hydrocarbon accumulation. *Bulletin, O.N.G.C.*, 27: 15-38.
- Sen, D. and Sen, S. 1983. Post-Neogene tectonism along the Aravalli range, Rajasthan, India. *Tectonophysics*, 93: 75-98.
- Schulz, H., Von Rad, U. and Erlenkeuser, H. 1998. Correlation between Arabian Sea and Greenland climate oscillations for the past 110,000 years. *Nature*, 393: 54-57.
- Schulz, H. and Emeis, K-C. 2002. The Toba volcanic event and interstadial/stadial climates at the marine isotopic stage 5 to 4 transition in the northern Indian Ocean. *Quaternary Research*, 57: 22-31.
- Shuster, M.W. and Steidtmann, J.R. 1987. Fluvial sandstone architecture and thrust

induced subsidence, northern Green river, Wyoming. In: F.G. Ethridge, R.M. Flores and M.D. Harvey (Eds.), *Recent Developments in Fluvial Sedimentology*. Special Publication, Society of Economic Paleontology and Mineralogy, 39: 279-285.

Sigurdsson, H. 1990. Evidence of volcanic loading of the atmosphere and climate response. *Palaeogeography, Palaeoclimatology, Palaeoecology*, 89: 277-289.

Singh, I.B. 1996. Geological evolution of Ganga Plain - an overview. *Journal of the Paleontological Society of India*, 41: 99-137.

Song, S. R., Chen, C. H., Lee, M. Y., Yang, T. F., Iizuka, Y. and Wei, K. Y. 2000. Newly discovered eastern dispersal of the youngest Toba Tuff. *Marine Geology*, 167: 303-312.

Tandon, S.K., Sareen, B.K., Someshwar Rao, M. and Singhvi, A.K. 1997. Aggradation history and luminescence chronology of the Sabarmati basin, Gujarat, Western India. *Palaeogeography, Palaeoclimatology, Palaeoecology*, 128: 339-357.

Todd, S.P. and Went, J.D. 1991. Lateral migration of sand bed rivers: Examples from the Devonian Glashabeg formation, SW Ireland and the Cambrian Alderney sandstone formation, Channel Islands. *Sedimentology*, 38: 997-1020.

Shankar, R. 1991. Thermal and crustal structure of 'SONATA': A zone of mid-continent rifting in Indian shield. *Journal of the Geological Society of India*, 37: 211-220.

Sridhar, A., Laskar, A., Prasad, V., Sharma, A., Tripathi, J., Balaji, D., Maurya, D.M. and Chamyal, L.S. 2015. Late Holocene flooding history of a tropical river in western India in response to southwest monsoon fluctuations: A multi-proxy study from lower Narmada valley. *Quaternary International*, 37: 181-190.

Srivastava, P., Juyal, N., Singhvi, A.K., Wasson, R.J. and Bateman, M.D. 2001. Luminescence chronology of river adjustment and incision of Quaternary sediments in the alluvial plain of the Sabarmati river, north Gujarat, India. *Geomorphology*, 36: 217-229.

Sunramanya, K.R. 1996. Active intraplate deformation in south India. *Tectonophysics*, 262: 231-241.

Thornes, J.B. 1994. Channel processes: Evolution and history. In, D.S.G. Thomas (Ed.), *Arid Zone Geomorphology*. John Wiley, Chichester, pp. 288-317.

Viseras, C. and Fernandez, J. 1995. The role of erosion and deposition in the construction of alluvial fan sequences in the Guadix Formation (SE Spain). *Geologieen Mijnbouw*, 74: 21-33.

Weaver, C.E. 1989. Clays, Muds and Shales. *Developments in Sedimentology*, 44. Elsevier, 819p.

Williams, M. A. J. and Clarke, M. F. 1984. Late Quaternary environments in north-central India. *Nature*, 308: 633-635.

Willis, B.J. and Beherensmeyer, A.K. 1994. Architecture of Miocene overbank deposits in Northern Pakistan. *Journal of Sedimentary Petrology*, B64 (1): 60-67.

Woodroffe, C.D., Chappell, J., Thom, B.G. and Wallensky, E. 1989. Depositional model of a microtidal estuary and floodplain, South Alligator river, northern Australia, *Sedimentology*, 36: 737-756.

Wright, L.D., Coleman, J.M. and Thom, B.G. 1973. Processes of channel development in a high-tide-range environment: Cambridge Golf-Ord River delta, Western Australia. *Journal of Geology*, 81: 15-41.

















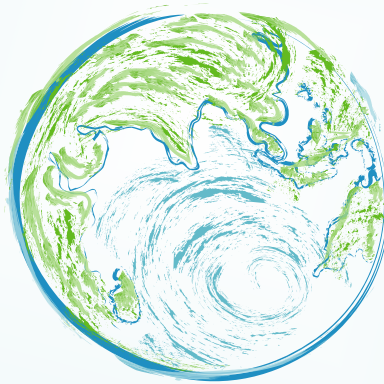
In collaboration with



Ministry of Earth Sciences  
Government of India



For Young Geomorphologists



[www.icg2017.com](http://www.icg2017.com)

